



## Evaluation of bioaccumulation of nanoplastics, carbon nanotubes, fullerenes, and graphene family materials

Elijah Petersen<sup>a,\*</sup>, Ana C. Barrios<sup>a</sup>, Rhema Bjorkland<sup>b</sup>, David G. Goodwin Jr<sup>c</sup>, Jennifer Li<sup>a</sup>, Greta Waissi<sup>d</sup>, Theodore Henry<sup>e</sup>

<sup>a</sup> Biosystems and Biomaterials Division, NIST, Gaithersburg, MD 20899, United States

<sup>b</sup> George Mason University, Fairfax, VA 22030, United States

<sup>c</sup> Engineering Laboratory, National Institute of Standards and Technology (NIST), Gaithersburg, MD 20899, United States

<sup>d</sup> University of Eastern Finland, School of Pharmacy, POB 1627 70211, Kuopio, Finland

<sup>e</sup> Institute of Life and Earth Sciences, School of Energy, Geoscience, Infrastructure and Society, Heriot-Watt University, Edinburgh EH14 4AS, United Kingdom

### ARTICLE INFO

#### Keywords:

Trophic transfer  
Nanoparticles  
Nanotechnology  
Engineered nanomaterials

### ABSTRACT

Bioaccumulation is a key factor in understanding the potential ecotoxicity of substances. While there are well-developed models and methods to evaluate bioaccumulation of dissolved organic and inorganic substances, it is substantially more challenging to assess bioaccumulation of particulate contaminants such as engineered carbon nanomaterials (CNMs; carbon nanotubes (CNTs), graphene family nanomaterials (GFNs), and fullerenes) and nanoplastics. In this study, the methods used to evaluate bioaccumulation of different CNMs and nanoplastics are critically reviewed. In plant studies, uptake of CNMs and nanoplastics into the roots and stems was observed. For multicellular organisms other than plants, absorbance across epithelial surfaces was typically limited. Biomagnification was not observed for CNTs and GFNs but were observed for nanoplastics in some studies. However, the reported absorption in many nanoplastic studies may be a consequence of an experimental artifact, namely release of the fluorescent probe from the plastic particles and subsequent uptake. We identify that additional work is needed to develop analytical methods to provide robust, orthogonal methods that can measure unlabeled (e.g., without isotopic or fluorescent labels) CNMs and nanoplastics.

### 1. Introduction

Bioaccumulation is a key indicator of potential adverse environmental effects given that persistence in an organism can lead to chronic toxicity. Moreover, understanding the bioaccumulation of substances supports the interpretation of toxicity test results: if substances are not bioavailable or do not accumulate, then any toxicity in internal organs may be indirect and a consequence of disruption of external tissue surfaces (e.g., disruption of respiratory, digestive system processes, or behavior/feeding).

Understanding the bioaccumulation of dissolved substances has well developed models and methods. In contrast, understanding the bioaccumulation of nano-sized particles is still under development. Engineered nanomaterials (ENMs) have a size in one dimension between 1 nm and 100 nm, (ASTM (American Society for Testing Materials) International, 2006; ISO (International Organization for Standardization), 2010) while nanoplastics are defined in a recent ISO standard (ISO,

2020) and have one size from 1 nm to 1000 nm. ENMs can and are being used in a wide range of potential commercial products (Burschka et al., 2013; Halamoda et al., 2019; Petersen et al., 2012; Sun et al., 2017), but their small size may also lead to environmental or human health risks upon release into the environment or exposure during product usage (Elliott et al., 2017; Hanna et al., 2016,2018; Klaine et al., 2008; Petersen et al., 2020; Roesslein et al., 2013). Important engineered carbon nanomaterials (CNMs) include carbon nanotubes (CNTs), fullerenes (and derivatized versions of them such as fullerlenols), and graphene family nanomaterials (GFNs), and also incidental particles such as nanoplastic particles formed as the result of the breakdown of plastic debris in the environment. Fullerenes typically consist of 60 or 70 sp<sup>2</sup>-hybridized carbon atoms arranged in a series of hexagons and pentagons to form a spherical structure, whereas CNTs have long tubular structures. GFNs, which include graphene, reduced graphene (rGO), few layer graphene (FLG), and graphene oxide (GO), consist of a single layer or a few layers of sp<sup>2</sup>-hybridized carbon with a sheet-like structure.

\* Corresponding author.

E-mail address: [elijah.petersen@nist.gov](mailto:elijah.petersen@nist.gov) (E. Petersen).

<https://doi.org/10.1016/j.envint.2022.107650>

Received 5 October 2022; Received in revised form 15 November 2022; Accepted 19 November 2022

Available online 21 November 2022

0160-4120/Published by Elsevier Ltd. This is an open access article under the CC BY license (<http://creativecommons.org/licenses/by/4.0/>).

Traditional approaches for estimating the bioaccumulation of organic chemicals, such as partitioning coefficients, have been shown to not be applicable to CNMs (Bjorkland et al., 2017; Petersen et al., 2010; Praetorius et al., 2014). Another substantial difference between the bioaccumulation behaviors of CNMs and nanoplastics and dissolved organic chemicals is that the larger size of CNMs and nanoplastics may not enable their passage across epithelial surfaces of organisms (Petersen et al., 2019b). In a review of CNT bioaccumulation studies published in 2017 (Bjorkland et al., 2017), a systematic trend was observed across a broad range of multicellular organisms (excluding plants): there was a lack of detectable absorption of CNTs across epithelial surfaces. In the few studies that evaluated trophic transfer of CNTs, biomagnification was not observed (Mortimer et al., 2016; Parks et al., 2013; Schierz et al., 2014). Similarly, a recent evaluation of the bioaccumulation of microplastic particles found that >99 % of the particles observed in field studies were in the organism gut tracts and not absorbed into their tissues (Gouin, 2020). However, it is not yet clear whether this trend would hold true across a broader range of CNMs and nanoplastics.

In this study, we have critically reviewed bioaccumulation studies of a range of CNMs and nanoplastics to evaluate the quality of the methods used and whether there are consistent trends. Given the range of different quantification approaches used among studies, the analytical methods for the different types of particles are then evaluated and results obtained using different analytical methods are compared. The methods for detecting the bioaccumulation of CNMs and nanoplastics are evolving, and the findings could be impacted by the method selected and its detection limit. Because bioaccumulation terminology can differ among studies, specific terminology from a recently published study on making robust nanoparticle (NP) bioaccumulation methods will be used (see the Supporting Information). Lastly, the bioaccumulation studies for each type of CNM and nanoplastics are critically evaluated with a focus on the use of control measurements to avoid potential artifacts. Our hypothesis is that the particle size of CNMs and nanoplastics will be more important for their bioaccumulation than the underlying chemical structure. In other words, similarly-sized nanoplastics and CNMs will have similar bioaccumulation behaviors. This is the reason why both CNMs and nanoplastics are evaluated here.

## 2. Methods for bioaccumulation evaluation

To identify publications on the bioaccumulation of CNTs (published since 2017), GFNs, fullerenes, and nanoplastics, we used an approach similar to that of a prior study (Bjorkland et al., 2017) by searching the Web of Science using a range of search terms, including, for example, “nanotube” and “bioaccumulation.” The most recent searches were performed in August 2021. We also sought out relevant review papers on the ecological risks of CNMs and nanoplastics, and reviewed the manuscripts cited in all papers for other potentially relevant studies. Papers were not removed from further analysis if they lacked key control experiments given the limited number of relevant studies, but these limitations were discussed in the text for selected papers that provided quantitative bioaccumulation values.

The methods used in bioaccumulation studies for the different types of CNMs and nanoplastics have been evaluated in terms of their frequency of use (Table 1 and Fig. 1). Information that might impact the bioaccumulation (e.g., detection method, particle size, exposure concentration, assay duration, test taxa and species) were extracted from the papers and organized into Tables 2–5. The presented CNT data in Table 2 only includes papers published after 2017 since a previous paper reviewed all 42 studies up that point (Bjorkland et al., 2017), although the new data was compared to that from the previous CNT bioaccumulation studies.

**Table 1**

The frequency of the main analytical techniques for different carbon nano-materials and nanoplastics.

Particle type	Method used in study	Percentage of studies using method (% (number using technique/total number of studies))
Carbon nanotubes	TEM	36 (18/50)
	<sup>14</sup> C labeling	34 (17/50)
	Raman spectroscopy	24 (12/50)
Graphene Family Nanomaterials	<sup>14</sup> C labeling	53 (9/17)
	TEM	24 (4/17)
	Raman spectroscopy	24 (4/17)
Fullerenes	TEM	52 (14/27)
	UV/vis spectroscopy	26 (7/27)
Nanoplastics	Light microscopy	26 (7/27)
	Fluorescence	73 (22/30)
	Light microscopy, TEM, SEM	7 each (2/30)

The studies analyzed are those in Fig. 1. Abbreviations: scanning electron microscopy (SEM), transmission electron microscopy (TEM).

## 3. Analytical methods

A primary challenge in understanding the bioaccumulation behaviors of CNMs and nanoplastics is that the analytical methods for quantifying their concentration in different tissues are still being developed and vary among studies (Fig. 1 and Table 1). However, comprehensive reviews of analytical methods for quantifying CNTs (Petersen et al., 2016), GFNs (Goodwin et al., 2018), fullerenes (Isaacson et al., 2009), and nanoplastics (Nguyen et al., 2019) have been published. Overall, quantitative measurements (measurements that can yield a concentration value and uncertainty) are superior to qualitative measurements (measurements that yield a “yes” or “no” answer), because they better enable comparisons among studies and use in risk assessment criteria. Some techniques yielded a relative concentration that enabled comparison among samples within the study (detected pixels corresponding to polystyrene (PS) particles in fish brain (Mattsson et al., 2017) or relative radioactive intensity (Soubaneh et al., 2020)) but cannot be readily linked to a concentration in units (e.g., mg/L) that enable comparisons to other studies. Such measurements are more limited than other quantitative measurements. Nevertheless, qualitative measurements using orthogonal methods can help confirm quantitative results (Petersen et al., 2019b). For example, detection of CNMs or nanoplastics in a tissue using a quantitative technique (e.g., quantification of the <sup>14</sup>C label) can be supported by an qualitative analysis (e.g., Raman microscopy) (Lu et al., 2017).

When feasible, it is best to analyze samples using orthogonal methods (i.e., those based on different measurement principles such as transmission electron microscopy (TEM) and detection of a radioactive label), because similar interferences or biases are less likely to impact orthogonal methods (Petersen et al., 2016). Unfortunately, few studies have been performed that directly compare orthogonal quantitative methods in complex matrices (e.g., comparing C<sup>14</sup> labeling and near IR fluorescence (NIRF) approaches to quantify single-wall CNTs (SWCNTs)) (Schierz et al., 2012). If differing results are obtained among orthogonal methods, efforts should be made to identify and resolve the cause of the disagreement. Depending upon the purpose of the study, it may be important to use multiple techniques that yield different information or multiple time points to assess gut avoidance and the elimination rate (Petersen et al., 2019b). The use of reference materials can help determine instrument or method performance for more mature research areas (e.g., metal concentration in a tissue such as NIST SRM 1566b (NIST, 2019)), but these are not yet available for emerging topics such as the bioaccumulation of CNMs and nanoplastics.

Bioaccumulation studies can have varying valid objectives and

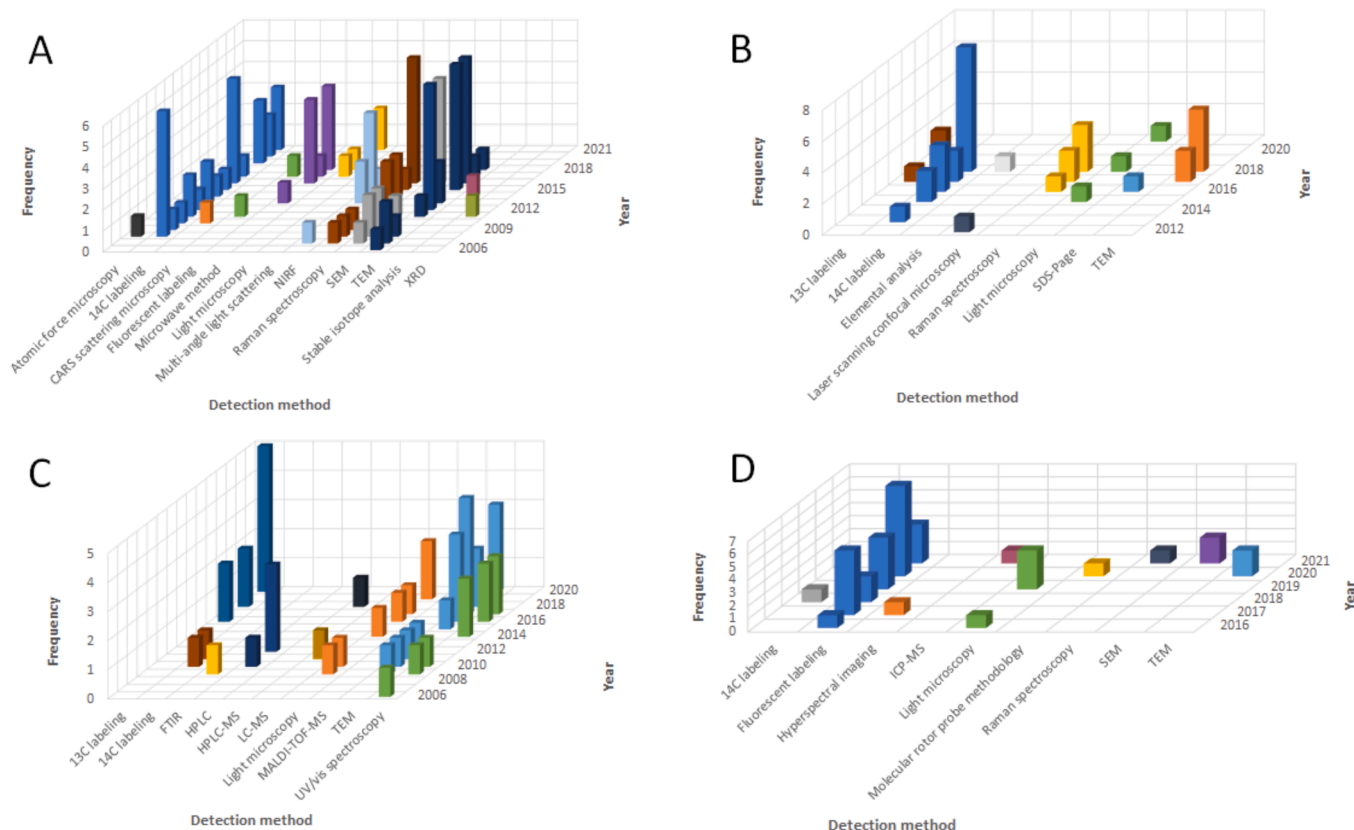


**Fig. 1.** Frequency of different detection methods used in bioaccumulation studies by year for (A) carbon nanotubes, (B) graphene family nanomaterials, (C) fullerenes and fullereneols, and (D) nanoplastics. Abbreviations: coherent anti-Stokes Raman spectroscopy (CARS), Fourier transform infrared spectroscopy (FTIR), high performance liquid chromatography (HPLC), inductively coupled plasma-mass spectrometry (ICP-MS), liquid chromatography-mass spectrometry (LC-MS), matrix assisted laser desorption/ionization-time of flight-mass spectrometry (MALDI-TOF-MS), near infrared fluorescence (NIRF), scanning electron microscopy (SEM), sodium dodecyl sulphate–polyacrylamide gel electrophoresis (SDS-PAGE), transmission electron microscopy (TEM), X-ray diffraction (XRD). This figure includes all studies described in tables 2 through 5 in addition to references from a prior publication on CNT bioaccumulation studies (Bjorkland et al., 2017). In some studies, multiple techniques were used. The total number of studies was 50, 17, 27, and 30 for CNTs, GFNs, fullerenes and fullereneols, and nanoplastics, respectively.

strategies for making robust and reproducible bioaccumulation studies with ENMs (Petersen et al., 2019b). A primary focus on bioaccumulation studies in this paper is the extent to which absorption across epithelial tissues occurs and the concentration in tissues other than the digestive tract, because this would yield results most similar to bioaccumulation studies for dissolved contaminants (Bjorkland et al., 2017). In the following sections, the advantages and limitations of the most commonly used techniques and potential artifacts (Petersen et al., 2019b) during their usage are briefly discussed. The most commonly used techniques for CNTs, GFNs, and nanoplastics do not require extraction from the biological matrix, while this is needed in only one of the three most common techniques for fullerenes (i.e., UV/vis spectroscopy). This topic is not thoroughly addressed here, because it has been investigated in depth in prior reviews (Petersen et al., 2016; Pycke et al., 2011,2012).

### 3.1. Carbon nanotubes (CNTs)

Unless the technique measures something unique to the type of CNT (e.g., NIRF analysis of SWCNTs (Petersen et al., 2016; Schierz et al., 2012)), the analytical technique can be used with different types of CNTs. The most frequently used method in studies with CNTs is TEM (35 % of the compiled studies; Table 1). This is a powerful technique that can theoretically identify a single nanoparticle in an entire organism. However, this technique can be challenging to use in practice with CNTs for many reasons. For example, there may be artifacts when attempting to distinguish between CNTs and other organic material. In one early

study, apparent absorption of CNTs into systemic circulation in *Daphnia magna* observed by TEM was determined to be an artifact based on subsequent analyses using high resolution TEM (HRTEM) and selected area electron diffraction (SAED) microscopy (Edgington et al., 2014). When electron microscopy is used to evaluate the bioaccumulation of CNMs or nanoplastics, it is important to carefully interrogate the particles observed using methods such as HRTEM to evaluate the material fine structure, SAED to evaluate the diffraction patterns, or electron energy loss spectroscopy (EELS) to evaluate the particle electronic structure (Edgington et al., 2014). These results can then be compared to analysis of the CNMs or nanoplastic after suspension in the test media to confirm that the bioaccumulated particles are those used in the experiment (Edgington et al., 2014). It is also important to evaluate if the sectioning process may have inadvertently removed CNTs that were in the tissue by evaluating if the cross-sections had any tears or if the diamond knife was damaged (Kobler et al., 2014). While electron microscopy (EM) is typically used to provide definitive CNT identification as a qualitative, confirmative method, there is an American Society of Testing and Materials (ASTM, 2015) method for quantifying asbestos that could be used for quantitative analysis. However, this method has not yet been used to evaluate CNM or nanoplastic bioaccumulation to our knowledge.

<sup>14</sup>C labeling followed by quantification of the <sup>14</sup>C label (e.g., using autoradiography (Al-Sid-Cheikh et al., 2020) or liquid scintillation counting (LSC) potentially after biological oxidation (Petersen et al., 2008a,b; Zhang et al., 2011,2012a)) is the second most commonly used method in studies on the bioaccumulation of CNTs (33 % of the

**Table 2**  
Summary of CNT bioaccumulation results published since 2017.

Type	Size	Functionalization	Detection method	Exposure	Concentration	Maximum Duration	Taxon	Species	Factor	Results	Reference
MWCNT	4 nm (inner); 5 nm to 20 nm (outer); $\geq 1$ $\mu\text{m}$ (avg. length)	$^{14}\text{C}$ labeling	$^{14}\text{C}$ labeling	Aqueous media (BG 11) and algal culture medium	$122 \mu\text{g L}^{-1}$	96 h	Algae	<i>Chlamydomonas reinhardtii</i>	BCF: 13 700 L $\text{kg}^{-1}$	Quantitative Maximum body burden: $1.6 \pm 0.4 \mu\text{g }^{14}\text{C-MWCNT mg}^{-1}$ (dry mass)	(Politowski et al., 2021)
MWCNT	4 nm (inner); 5 nm to 20 nm (outer); $\geq 1$ $\mu\text{m}$ (avg. length)	$^{14}\text{C}$ labeling	$^{14}\text{C}$ labeling	Algal culture medium	$123 \mu\text{g L}^{-1}$	96 h	Algae	<i>Raphidocelis subcapitata</i>	BCF: 6800 L $\text{kg}^{-1}$	Quantitative Maximum body burden: $0.7 \pm 0.3 \mu\text{g }^{14}\text{C-MWCNT mg}^{-1}$ (dry mass)	(Politowski et al., 2021)
MWCNT	110 nm to 170 nm outer diameter, 5 $\mu\text{m}$ to 9 $\mu\text{m}$ length	$^{14}\text{C}$ labeled ethanolamine	$^{14}\text{C}$ labeling	Filtered (0.2 $\mu\text{m}$ ) freshwater	$160 \text{ mg L}^{-1}$	3 h	Fish	<i>Salvelinus alpinus</i>		Qualitative Radioactivity pattern showed accumulation in head bone canals; in contrast, free [ $^{14}\text{C}$ ]-labeled ethanolamine accumulated in the olfactory bulb, gills, liver, and pyloric caeca and not in head bones	(Soubaneh et al., 2020)
MWCNT	30 nm to 50 nm outer diameter, 10 $\mu\text{m}$ to 20 $\mu\text{m}$ length	$^{14}\text{C}$ labeled ethanolamine	$^{14}\text{C}$ labeling	Filtered (0.2 $\mu\text{m}$ ) freshwater	$90 \text{ mg L}^{-1}$	3 h	Fish	<i>Salvelinus alpinus</i>		Quantitative There was less accumulation of [ $^{14}\text{C}$ ]-labeled ethanolamine than with the shorter, thicker MWCNTs	(Soubaneh et al., 2020)
MWCNT	20 nm to 30 nm, outer diameter	None	Microwave method	Dietary ( <i>D. magna</i> fed CNTs stabilized in SDBS)	$0.1 \text{ mg L}^{-1}$	7 d	Fish	<i>Pimephales promelas</i>	BAF: 2.7 L $\text{kg}^{-1}$	Quantitative Fathead minnow MWCNT accumulation was $0.04 \pm 0.11 \mu\text{g g}^{-1}$ ; distribution throughout the fish was not determined	(Cano et al., 2018)
MWCNT	8 nm to 15 nm, outer diameter	None	Microwave method	Dietary ( <i>D. magna</i> fed CNTs stabilized in SDBS)	$0.1 \text{ mg L}^{-1}$	7 d	Fish	<i>Pimephales promelas</i>	BAF: 19.2 L $\text{kg}^{-1}$	Quantitative Fathead minnow MWCNT accumulation was $0.81 \pm 0.19 \mu\text{g g}^{-1}$ ; distribution throughout the fish was not determined	(Cano et al., 2018)
MWCNT	36.5 nm diameter; 353 nm length	$^{14}\text{C}$ labeling	$^{14}\text{C}$ labeling	Aqueous (Hoagland media)	$2.25 \text{ mg L}^{-1}$	24 h	Legumes	<i>Glycine max</i>		Quantitative MWCNTs translocated to above-ground tissue, up to $76.6 \text{ mg kg}^{-1}$ (in soybean root); highest levels were found in root tissue.	(Zhao et al., 2017b)
MWCNT	36.5 nm diameter; 353 nm length	$^{14}\text{C}$ labeling	$^{14}\text{C}$ labeling	Aqueous (Hoagland media)	$2.25 \text{ mg L}^{-1}$	24 h	Monocot	<i>Oryza sativa L.</i>		Quantitative The MWCNTs content in rice root was approximately $22.5 \text{ mg kg}^{-1}$ , two-fold the amount in the sheath; rice was found to translocate more MWCNTs to the above ground tissues (leaf and sheath) as compared to <i>Arabidopsis</i> , maize, and corn	(Zhao et al., 2017b)

(continued on next page)

Table 2 (continued)

Type	Size	Functionalization	Detection method	Exposure	Concentration	Maximum Duration	Taxon	Species	Factor	Results	Reference
MWCNT	36.5 nm diameter; 353 nm length	<sup>14</sup> C labeling	<sup>14</sup> C labeling	Aqueous (Hoagland media)	2.25 mg L <sup>-1</sup>	24 h	Monocot	<i>Zea mays</i>		Quantitative MWCNTs translocated to above-ground tissue, (0.53 mg kg <sup>-1</sup> ); highest levels were found in root tissue	(Zhao et al., 2017b)
MWCNT	4 nm inner diameter; 5 nm to 20 nm diameter, outer, > 1 μ length	<sup>14</sup> C labeled	<sup>14</sup> C labeling	Released material from irradiated and mechanically stressed epoxy nanocomposite in quartz sand and reconstituted water medium	0.838 μg released MWCNT in 8 g quartz sand and 24 mL reconstituted water	48 h	Oligochaete	<i>Lumbriculus variegatus</i>	BSAF: 0.020 ± 0.010	Quantitative 66% of the MWCNTs was eliminated again after 24 h after exposure to released particles from a nanocomposite	(Hennig et al., 2019)
MWCNT	4 nm inner diameter; 5 nm to 20 nm diameter, outer, > 1 μ length	<sup>14</sup> C labeling	<sup>14</sup> C labeling	MWCNT mixed in reconstituted water which was poured over quartz sand	845 ng L <sup>-1</sup> sand and 24 mL reconstituted water	48 h	Oligochaete	<i>Lumbriculus variegatus</i>	BSAF: 0.003 ± 0.001.	Quantitative 96% of the ingested material was eliminated after 24 h	(Hennig et al., 2019)
MWCNT	4 nm inner diameter; 5 nm to 20 nm diameter, outer, > 1 μ length	<sup>14</sup> C labeling	<sup>14</sup> C labeling	MWCNT mixed in quartz sand, which was overlaid with reconstituted water	845 ng L <sup>-1</sup> sand and 24 mL reconstituted water	48 h	Oligochaete	<i>Lumbriculus variegatus</i>	BSAF: 0.020 ± 0.018	Quantitative 75 % of the ingested material eliminated after 24 h	(Hennig et al., 2019)
MWCNT	8 nm to 15 nm (outer diameter), 10 μm to 50 μm (length) or 20 nm to 30 nm (outer diameter), 10 μm to 30 μm (length)	None, but CNTs stabilized in sodium dodecyl benzenesulfonate (SDBS)	Microwave method	Aqueous media (MHW)	0.1 mg L <sup>-1</sup>	3 d	Planktonic crustacean	<i>Daphnia magna</i>	BCF: 0.24 L kg <sup>-1</sup> and 0.55 L kg <sup>-1</sup> for the narrower and larger diameter MWCNTs, respectively	Quantitative <i>D. magna</i> MWCNT accumulation was 0.02 μg g <sup>-1</sup> and 0.06 μg g <sup>-1</sup> for the narrower and larger diameter MWCNTs, respectively	(Cano et al., 2018)
MWCNT	8 nm to 15-nm (outer diameter), 10 μm to 50 μm length or 20 nm to 30 nm (outer diameter), 10 μm to 30 μm length	None, but CNTs stabilized in SDBS	Microwave method	Aqueous media (MHW and HW)	0.1 mg L <sup>-1</sup>	3 d	Planktonic crustacean	<i>Daphnia magna</i>		Quantitative Higher concentrations of MWCNTs accumulated in <i>D. magna</i> exposed in hard freshwater; however, no significant differences were observed between bioaccumulation of MWCNTs with varying diameter sizes	(Cano et al., 2017)
MWCNT	4 nm (inner); 5 nm to 20 nm (outer); ≥1	<sup>14</sup> C labeling	<sup>14</sup> C labeling, light microscopy	Weathered In aqueous media	100 μg <sup>14</sup> C-wMWCNT L <sup>-1</sup>	72 h	Planktonic crustacean	<i>Daphnia magna</i>	BCF: 140 000 BAF: 120	Quantitative Maximum body burden: 0.07 μg MWCNT mg <sup>-1</sup> dw <sup>-1</sup>	(Politowski et al., 2021)

(continued on next page)

Table 2 (continued)

Type	Size	Functionalization	Detection method	Exposure	Concentration	Maximum Duration	Taxon	Species	Factor	Results	Reference
	$\mu\text{m}$ (avg. length)			(M4 media) (with and without algae)						and $7.1 \mu\text{g}^{14}\text{C-MWCNT mg}^{-1}\text{dw}^{-1}$ (with algae and without, respectively); complete elimination observed after exposure through algae	
MWCNT	4 nm (inner); 5 nm to 20 nm (outer); $\geq 1 \mu\text{m}$ (avg. length)	$^{14}\text{C}$ labeling	$^{14}\text{C}$ labeling	Weathered (w) In aqueous media (M4 Media)		28 d	Planktonic crustacean	<i>Daphnia magna</i>	BAF: $6700 \pm 2900 \text{ L kg}^{-1}$	Quantitative Maximum body burden of $0.7 \mu\text{g mg}^{-1} \text{ dw}^{-1}$	(Politowski et al., 2021)
MWCNT	21 nm (avg. diameter); $10 \mu\text{m}$ to $20 \mu\text{m}$ (avg. length)	Suspended in alginic acid	Light microscopy	Dryl's medium	$10 \text{ mg L}^{-1}$	1 h	Protozoa	<i>Tetrahymena Thermophila</i>	Calculated BCF: $755 \text{ L kg}^{-1}$	Quantitative Significant uptake during 1 h exposure; complete elimination occurred by 24 h	(Mortimer et al., 2021)
MWCNT	36.5 nm (avg. diameter); 353 nm (avg. length)	$^{14}\text{C}$ labeling	$^{14}\text{C}$ labeling	Aqueous (Hoagland media)	$2.25 \text{ mg L}^{-1}$	24 h	Rosid	<i>Arabidopsis thaliana</i>		Quantitative The MWCNT content in <i>Arabidopsis</i> leaf ( $13.0 \text{ mg kg}^{-1}$ ) was the highest among four plants	(Zhao et al., 2017b)
MWCNT	5 nm to 15 nm (outer diameter), 3 nm to 10 nm (inner diameter), $10 \mu\text{m}$ to $30 \mu\text{m}$ length	Oxidized, fluorescein isothiocyanate (FITC)-labeled MWCNT	Light microscopy, fluorescent labeling, TEM	Filtered natural sea water (FNSW)	$50 \text{ mg L}^{-1}$	48 h	Zooplanktonic crustacean	<i>Artemia salina</i> newly hatched larvae		Quantitative O-MWCNTs distributed in phagocyte, lipid vesicle and intestines; the majority of the MWCNTs were excreted after 72 h in FNSW	(Zhu et al., 2017)
SWCNT	279 nm, avg. length	Oxidized (O-SWCNT)	Light microscopy, TEM, Raman spectroscopy	Filtered natural sea water (FNSW)	$25 \text{ mg L}^{-1}$ to $600 \text{ mg L}^{-1}$	48 h	Zooplanktonic crustacean	<i>Artemia salina</i>		Quantitative O-SWCNT content increased from 1 h to 48 h followed by a decrease from 48 h to 72 h O-SWCNT accumulated in the gut tract, lipid vesicles and phagocytes; body burdens were in the range from $0.08$ to $5.7 \text{ mg g}^{-1}$ ; incomplete elimination after a 24 h in FNSW	(Zhu et al., 2018)

Abbreviations: bioaccumulation factor (BAF), bioconcentration factor (BCF), biota sediment accumulation factor: (BSAF), filtered natural sea water (FNSW), fluorescein isothiocyanate (FITC), hard water (HW), moderately hard water (MHW), multiwall carbon nanotubes (MWCNT), single-walled carbon nanotubes (SWCNT), transmission electron microscopy (TEM).

**Table 3**  
Summary of graphene family nanomaterial bioaccumulation results.

Type	Size	Functionalization	Detection method	Exposure	Concentration	Maximum Duration	Taxon	Species	Factor	Results	Reference
FLG	60 nm to 590 nm; height of 1 nm to 4 nm		<sup>14</sup> C labeling, TEM, Raman spectroscopy	Aqueous media (artificial freshwater)	0.1 mg L <sup>-1</sup> , 1 mg L <sup>-1</sup>	24 h	Algae	<i>Scenedesmus obliquus</i>		Quantitative Maximum concentration associated with cells was 320 ng/10 <sup>6</sup> cells; graphene was detected outside and inside cells	(Su et al., 2018b)
FLG	Peaks of 300 nm and 2000 nm (hydrodynamic diameter); height of mainly 4 layers		<sup>14</sup> C labeling	Aqueous media (Luria broth medium)	0.05 mg L <sup>-1</sup> to 1 mg L <sup>-1</sup>	2 h	Bacteria	<i>Escherichia coli</i>	BCF <sup>b</sup> : 2198	Quantitative Maximum uptake was 0.952 ng/cell	(Dong et al., 2018)
FLG	Peaks of 300 nm and 2000 nm (hydrodynamic diameter); height of mainly 4 layers		<sup>14</sup> C labeling	Aqueous media (artificial freshwater; direct exposure in water or trophic transfer via <i>D. magna</i> )	0.001 mg L <sup>-1</sup> , 0.05 mg L <sup>-1</sup> (water exposure); 10 <i>D magna</i> (1.38 g kg <sup>-1</sup> daily for trophic transfer)	28 d	Fish	<i>Danio rerio</i>	BBF <sup>b</sup> : ≈ 32; BMF <sup>b</sup> : 0.014	Quantitative Maximum uptake was ≈ 16 mg kg <sup>-1</sup> (trophic transfer) and ≈ 8 mg kg <sup>-1</sup> (water exposure)	(Dong et al., 2018)
FLG	60 nm to 590 nm; height of 1 nm to 4 nm	Suspended with or without algae	<sup>14</sup> C labeling, TEM, Raman spectroscopy	Aqueous media (artificial freshwater; with and without algae)	0.061 mg L <sup>-1</sup> (no algae), 0.046 mg L <sup>-1</sup> , 0.035 mg L <sup>-1</sup> (with algae)	48 h	Gastropod mollusc	<i>Cipangopaludina cathayensis</i>	BCF <sup>b</sup> : 20 to 200 (no algae), BAF: 2700 (with algae)	Quantitative Maximum uptake for the whole body was ≈ 16 mg kg <sup>-1</sup> (with algae; dry mass); uptake was highest in the intestine; in algae exposure, 1.3 % of FLG mass was in the liver	(Su et al., 2018b)
FLG	60 nm to 590 nm; height of 1 nm to 4 nm	With or without alginate present	<sup>14</sup> C labeling, TEM, Raman spectroscopy	Aqueous media (artificial freshwater)	0.158 mg L <sup>-1</sup>	72 h	Gastropod mollusc	<i>Cipangopaludina cathayensis</i>		Quantitative Maximum uptake for whole body was ≈ 16 mg kg <sup>-1</sup> (dry mass); uptake was highest in the intestine and gills; FLG observed in intestinal epithelial cells	(Su et al., 2018a)
FLG	60 to 120 nm; height of 1.05 nm	<sup>14</sup> C labeling; with and without natural organic matter (NOM)	<sup>14</sup> C labeling, TEM	Aqueous medium (25 % nutrient solution)	0.05 mg L <sup>-1</sup> to 0.5 mg L <sup>-1</sup>	21 d	Monocot (rice)	<i>Oryza sativa</i> L.		Quantitative Highest uptake amount in roots was 695 mg kg <sup>-1</sup> and in shoots was 54 mg kg <sup>-1</sup> ; full removal of the FLG in the shoots and leaves occurred after 75 d in soil; for FLG wrapped in NOM during the uptake period, only 15 % remained in the	(Huang et al., 2018)

(continued on next page)

Table 3 (continued)

Type	Size	Functionalization	Detection method	Exposure	Concentration	Maximum Duration	Taxon	Species	Factor	Results	Reference
FLG	60 nm to 590 nm; height of 1 nm to 4 nm	Uncoated, or coated with BSA	<sup>14</sup> C labeling	Aqueous media (artificial freshwater)	0.1 mg L <sup>-1</sup> to 1 mg L <sup>-1</sup>	48 h	Oligochaete	<i>Limnodrilus hoffmeisteri</i>		stem and leaves after 45 d of elimination Quantitative Maximum uptake for uncoated FLG was 60 mg kg <sup>-1</sup> (dry mass); uptake was approximately a factor of ten greater for BSA-coated FLG; after 12 h elimination in clean freshwater, the remaining concentration was 1.54 mg kg <sup>-1</sup> (>90 % elimination)	(Mao et al., 2016)
FLG	60 nm to 590 nm; height of 1 nm to 4 nm	Uncoated, BSA-coated, or coated from proteins after exposure with <i>L. hoffmeisteri</i>	<sup>14</sup> C labeling	Topsoil (Nanjing, China)	1 mg kg <sup>-1</sup>	21 d	Oligochaete	<i>Eisenia foetida</i>	BAF (protein coated): ≈ 0.125; BAF (uncoated) ≈ 0.05	Quantitative BAF values for uncoated FLG were similar to those for a non-bioaccumulating substance only in the earthworm gut tract; protein-coated FLG was greater than this amount	(Mao et al., 2016)
FLG	60 nm to 590 nm; height of 1 nm to 4 nm	<sup>14</sup> C labeling	<sup>14</sup> C labeling	Aqueous media (artificial freshwater)	0.5 mg L <sup>-1</sup> (with and without Fenton reaction)	24 h	Planktonic crustacean	<i>Daphnia magna</i>		Quantitative Highest uptake amount was 17 g kg <sup>-1</sup> (dry mass; 24 h) for unreacted FLG; FLG after Fenton reaction had values that were nearly 2 orders of magnitude lower	(Feng et al., 2015)
FLG	Peaks of 300 nm and 2000 nm (hydrodynamic diameter); height of 4 layers	<sup>14</sup> C labeling	<sup>14</sup> C labeling	Aqueous media (artificial freshwater)	0.025 mg L <sup>-1</sup> to 0.25 mg L <sup>-1</sup>	48 h	Planktonic crustacean	<i>Daphnia magna</i>		Quantitative Highest uptake was 7.8 g kg <sup>-1</sup> (dry mass; 24 h); elimination was complete after 1 h to 4 h if algae feeding was available	(Guo et al., 2013)
FLG	60 nm to 590 nm; height of 1 nm to 4 nm	<sup>14</sup> C labeling	<sup>14</sup> C labeling	Aqueous media (artificial freshwater)	0.25 mg L <sup>-1</sup> (with and without peroxidase catalyzed reaction with tetrabromobisphenol A)	48 h	Planktonic crustacean	<i>Daphnia magna</i>		Quantitative Highest uptake amount was 7.5 mg kg <sup>-1</sup> for the unreacted FLG; uptake was approximately a factor of two less for the reacted FLG	(Lu et al., 2015)
FLG	60 nm to 590 nm; height of 1 nm to 4 nm	Uncoated, BSA-coated, or coated from proteins after exposure	<sup>14</sup> C labeling	Aqueous media (artificial freshwater)	0.1 mg L <sup>-1</sup>	48 h	Planktonic crustacean	<i>Daphnia magna</i>		Quantitative Maximum uptake was 4.8 g kg <sup>-1</sup> (dry mass); uptake of protein-	(Mao et al., 2016)

(continued on next page)

Table 3 (continued)

Type	Size	Functionalization	Detection method	Exposure	Concentration	Maximum Duration	Taxon	Species	Factor	Results	Reference
		with <i>L. hoffmeisteri</i>								coated and BSA-coated FLG was typically a factor of 2 less	
FLG	Peaks of 300 nm and 2000 nm (hydrodynamic diameter) height of mainly 4 layers		<sup>14</sup> C labeling	Aqueous media (artificial freshwater; direct exposure in water or trophic transfer via <i>T. thermophila</i> )	0.0025 mg L <sup>-1</sup> , 0.25 mg L <sup>-1</sup> (water exposure); 0.0245 mg L <sup>-1</sup> (trophic transfer)	20 h	Planktonic crustacean	<i>Daphnia magna</i>	BBF <sup>b</sup> : 7783; BMF: 0.013	Quantitative Body burden values were higher for trophic transfer than for direct exposure for a similar suspended FLG concentration; however, biomagnification was unlikely to have occurred	(Dong et al., 2018)
FLG	Peaks of 300 nm and 2000 nm (hydrodynamic diameter); height of mainly 4 layers		<sup>14</sup> C labeling	Aqueous media (1 % SSP media; exposed by <i>E. coli</i> and water only)	0.1 mg L <sup>-1</sup> , 0.25 mg L <sup>-1</sup> (water only); 0.137 mg L <sup>-1</sup> (trophic transfer)	22 h	Protozoa	<i>Tetrahymena thermophila</i>	BCF <sup>b</sup> : 126,000; BMF: 8.57	Quantitative Uptake was higher for the direct exposure (0.1 mg L <sup>-1</sup> ) than for trophic transfer (0.0137 mg L <sup>-1</sup> )	(Dong et al., 2018)
Graphene nanoplatelets	1225 nm (avg. diameter); 5 nm (avg. thickness)	Suspended in alginic acid	Light microscopy	Dryl's medium	10 mg L <sup>-1</sup>	1 h	Protozoa	<i>Tetrahymena Thermophila</i>	Calculated BCF: 287 L kg <sup>-1</sup>	Quantitative Significant uptake during 1 h exposure (body burden 3800 mg kg <sup>-1</sup> dw); ≈ 99 % elimination occurred by 24 h	(Mortimer et al., 2021)
GO	200 nm to 8000 nm; 1 to 5 layers thick		Light microscopy	Aqueous media (added nutritive salts)	0.05 mg L <sup>-1</sup> to 50 mg L <sup>-1</sup>	12 d	Amphibian	<i>Xenopus laevis</i>		Qualitative GO agglomerates observed in the larvae gills and digestive tract in a dose-dependent manner	(Lagier et al., 2017)
GO	500 nm to 5000 nm; predominately single layer		Light microscopy, SEM	Aqueous media (filtered natural sea water)	10 mg L <sup>-1</sup>	48 h	Brachiopod crustacean	<i>Artemia salina</i>		Qualitative GO was visually observed in the gut tract and also on the membrane surface, gills, and abdomen using electron microscopy	(Mesaric et al., 2015)
GO	Unclear	<sup>13</sup> C labeling	<sup>13</sup> C labeling, IRMS	Aqueous medium (Hoagland nutrient solution)	0.6 mg L <sup>-1</sup>	20 d	Legumes (peas)	<i>Pisum sativum</i> L.		Quantitative Highest amount of uptake in any tissue was in the roots (1299 mg kg <sup>-1</sup> ); maximum uptake in leaves was approximately a factor of 4 lower	(Chen et al., 2019)
GO	Unclear length and width;	Acid washing, sonication; <sup>13</sup> C labeling	<sup>13</sup> C labeling, IRMS	Aqueous medium (Hoagland nutrient solution)	1 mg L <sup>-1</sup>	15 d	Monocot (wheat)	<i>Triticum aestivum</i>	0.71 % of exposed dosage per	Quantitative Uptake detected into roots; uptake	(Chen et al., 2017a)

(continued on next page)

Table 3 (continued)

Type	Size	Functionalization	Detection method	Exposure	Concentration	Maximum Duration	Taxon	Species	Factor	Results	Reference
	height of roughly 0.9 nm								gram in roots (7 d)	concentration decreased with exposure time; uptake into stem and leaves was not statistically different from control	
GO	106 nm hydrodynamic diameter; height of 1 nm	Coated with FITC/PEG/poly-L-lysine	Laser scanning confocal microscopy	Aqueous media	20 mg L <sup>-1</sup>	4 h	Nematode	<i>Caenorhabditis elegans</i>		Qualitative GO was observed along the length of the worm's body and also in the anterior part of the intestine	(Zhang et al., 2012b)
GO	200 nm to 300 nm; height of 1 nm	None	Elemental analysis	Aqueous media (daphnia culture medium)	5 mg L <sup>-1</sup> , 10 mg L <sup>-1</sup>	24 h	Planktonic crustacean	<i>Daphnia magna</i>	BCF (5 mg L <sup>-1</sup> ): 23,280; BCF (10 mg L <sup>-1</sup> ): 13,002	Quantitative Highest uptake amount was 113.9 g kg <sup>-1</sup> (dry weight); almost all GO was removed during 24 h elimination period	(Lv et al., 2018)
Graphene	0.5 μm to 2 μm; height of 0.76 nm	None	SDS-Page, micro-Raman microscopy	Aqueous medium (SM7 with polyvinylpyrrolidone added as a surfactant)	0.1 mg L <sup>-1</sup> to 1 mg L <sup>-1</sup>	21 d	Planktonic crustacean	<i>Daphnia magna</i>		Quantitative Uptake was 90.7 mg kg <sup>-1</sup> (wet mass; 1 mg L <sup>-1</sup> exposure concentration); below detection limit (0.15 μg) for the 0.1 mg L <sup>-1</sup> and 0.5 mg L <sup>-1</sup> exposure concentrations	(Fan et al., 2016)
Large FLG	300 nm to 700 nm; height of 1.4 nm	<sup>14</sup> C labeling; with and without NOM	<sup>14</sup> C labeling, TEM, Raman spectroscopy	Aqueous media (freshwater)	0.05 mg L <sup>-1</sup> to 0.25 mg L <sup>-1</sup>	72 h	Fish	<i>Danio rerio</i>		Quantitative Highest uptake amount was ≈ 100 mg kg <sup>-1</sup> (dry mass) with NOM; uptake was less without NOM; complete elimination observed after 12 h for FLG without NOM, while elimination was 92 % for FLG with NOM after 72 h; dissection revealed FLG only in the gut tract and gills	(Lu et al., 2017)
rGO	Unclear	Reduction performed using vitamin C; <sup>13</sup> C labeling	<sup>13</sup> C labeling, IRMS	Aqueous medium (Hoagland nutrient solution)	0.66 g L <sup>-1</sup>	20 d	Legumes (peas)	<i>Pisum sativum</i> L.		Quantitative Highest amount of uptake in any tissue was in the leaves (1822 ± 95 mg kg <sup>-1</sup> ); uptake was not observed in stems or	(Chen et al., 2019)

(continued on next page)

Table 3 (continued)

Type	Size	Functionalization	Detection method	Exposure	Concentration	Maximum Duration	Taxon	Species	Factor	Results	Reference
Small FLG	20 nm to 70 nm; height of 1.05 nm	<sup>14</sup> C labeling; with and without NOM	<sup>14</sup> C labeling, TEM, Raman spectroscopy	Aqueous media (freshwater)	0.05 mg L <sup>-1</sup> to 0.25 mg L <sup>-1</sup>	72 h	Fish	<i>Danio rerio</i>		leaves at 10 d, but higher amounts were observed at 15 d and 20 d Quantitative Highest uptake amount was ≈ 5 mg kg <sup>-1</sup> (dry mass) with NOM; uptake was up to two orders of magnitude less without NOM; only 30 % was depurated after 68 h for FLG without NOM and up to 80 % removed for FLG with NOM; dissection revealed detectable FLG in the gut and liver	(Lu et al., 2017)

a: The authors call this BAF although this is done in a liquid media with and without food. Also, units are converted from L g<sup>-1</sup> to L kg<sup>-1</sup>.

b: The authors refer to these as body burden factors but were calculated similarly to traditional BCF factors.

Abbreviations: bioconcentration factor (BCF), biomagnification factor (BMF), bovine serum albumin (BSA), fluorescein isothiocyanate (FITC), few layer graphene (FLG), graphene oxide (GO), isotope ratio mass spectrometry (IRMS), natural organic matter (NOM), polyethylene glycol (PEG), reduced graphene oxide (rGO), scanning electron microscopy (SEM), sodium dodecyl sulphate–polyacrylamide gel electrophoresis (SDS-PAGE), transmission electron microscopy (TEM).

**Table 4**  
Summary of fullerene and fullerene bioaccumulation results.

Type	Average Size	Dispersion method	Detection method	Exposure	Concentration	Maximum Duration	Taxon	Species	Factor	Results	Reference
Fullerene (C <sub>60</sub> and C <sub>70</sub> )	565 nm (C <sub>60</sub> ), 6459 nm (C <sub>70</sub> )	Water stirring	Light microscopy	Synthetic freshwater	5 mg L <sup>-1</sup> to 50 mg L <sup>-1</sup> (acute toxicity test), 7 mg L <sup>-1</sup> (21-d exposure)	21 d	Planktonic crustacean	<i>Daphnia magna</i> and <i>Daphnia pulex</i>		Qualitative Observations for darkening of the carapace and gut.	(Moore et al., 2019)
Fullerene (C <sub>60</sub> )	208 nm or 179 nm with or without humic acid, respectively	Toluene-water exchange method	UV/vis spectroscopy, TEM	Waterborne exposure (SE medium) with and without humic acid	2 mg L <sup>-1</sup>	24 h uptake, and 24 h elimination	Algae	<i>Scenedesmus obliquus</i>		Quantitative Body burden of 227 mg kg <sup>-1</sup> or 246 mg kg <sup>-1</sup> (wet weight) without or with humic acid, respectively; nearly complete elimination (up to 94 %); using TEM, particles were observed on and in cells	(Chen et al., 2016)
Fullerene (C <sub>60</sub> )	162 nm (t = 0d), 215 nm (t = 9 d)	Water stirring	HPLC-MS	Waterborne exposure	1.0 µg L <sup>-1</sup>	72 h	Biofilm	<i>Biofilm</i>	BCF: 1.34 (dry mass)	Quantitative Similar BCF values for fullerenes and one of their degradation products	(Sanchis et al., 2020)
Fullerene (C <sub>60</sub> )	40 nm to 600 nm	Water stirring	HPLC-MS	Algal suspension	1.9 ng L <sup>-1</sup> to 5.1 ng L <sup>-1</sup>	21 d of exposure and 7 d elimination	Bivalve mollusc (marine)	<i>Mytilus galloprovincialis</i>		Quantitative Maximum uptake was 12.1 µg kg <sup>-1</sup> (wet weight); after 7 d elimination, it decreased to 9.3 µg kg <sup>-1</sup>	(Sanchis et al., 2018)
Fullerene (C <sub>60</sub> )	490 nm	Water stirring	TEM	Settling from overlying water onto sediment	0.36 mg cm <sup>-2</sup> to 0.55 mg cm <sup>-2</sup> (mass/sediment surface)	10-d	Dipterid	<i>Chironomus riparius</i>		Qualitative Agglomerates were observed in the gut, but no absorption into the gut epithelial cells was detected	(Waissi-Leinonen et al., 2012)
Fullerene (C <sub>60</sub> )	515 nm	Water stirring	TEM	Spiked sediment	0.0004 mg kg <sup>-1</sup> to 80 mg kg <sup>-1</sup>	10-d chronic test and emergence test	Dipterid	<i>Chironomus riparius</i>		Qualitative Agglomerates were observed in the gut, no absorption into the gut epithelial cells	(Waissi-Leinonen et al., 2015)
Fullerene (C <sub>60</sub> )	Approximately 500 nm to 1000 nm	Water stirring	UV/vis spectroscopy, TEM	Settling from overlying water onto sediment	0.025 mg cm <sup>-2</sup> to 0.48 mg cm <sup>-2</sup> (mass/sediment surface)	28 d	Dipterid	<i>Chironomus riparius</i>		Quantitative Maximum uptake is 4.85 mg kg <sup>-1</sup> (wet mass); decreased concentrations with longer exposure periods; absorption into the gut epithelial cells was not detected	(Waissi et al., 2017a)
Fullerene (C <sub>60</sub> )	367 nm to 515 nm	Water stirring	TEM	Spiked sediment	0.5 mg kg <sup>-1</sup> to 40 mg kg <sup>-1</sup> (dry mass)	34 d	Dipterid	<i>Chironomus riparius</i>		Qualitative Agglomerates known to be observed in the gut, but absorption into the gut epithelial cells was not detected	(Waissi et al., 2017b)
Fullerene (C <sub>60</sub> )	NA	40 mg of C <sub>60</sub> fullerenes were added to 12 g of vermiculite	HPLC	Soil	1000 mg L <sup>-1</sup>	20d	Eudicot	<i>Solanum lycopersicum L.</i>		Quantitative Fullerenes were detected in the roots (1760 µg kg <sup>-1</sup> ) but were not detected in the shoots	(De La Torre-Roche et al., 2012)

(continued on next page)

Table 4 (continued)

Type	Average Size	Dispersion method	Detection method	Exposure	Concentration	Maximum Duration	Taxon	Species	Factor	Results	Reference
Fullerene (C <sub>60</sub> )	50 % were less than 100 nm while 40 % were >1500 nm	Solvent exchange with tetrahydrofuran	C-14 labelling	Addition to sand or hydroponic exposure	8.44 mg L <sup>-1</sup>	16 d	Eudicot (radish)	<i>Raphanus sativus</i>		Quantitative Plant uptake was ~7% with similar uptake for sand and hydroponic exposure; most accumulation was in the roots (40 % to 47 %) with smaller amounts in the tubes, stems, and leaves	(Avanasi et al., 2014)
Fullerene (C <sub>60</sub> )	139 nm (DLS); 57.6 nm (TEM)	Solvent exchange method with toluene and ethanol	UV/vis spectroscopy	Artificial freshwater with and without humic acid	0.2 mg L <sup>-1</sup> , 2 mg L <sup>-1</sup>	3 d uptake and 48 h elimination	Fish	<i>Danio rerio</i>		Quantitative Modeled maximum body burden: 222 ± 30 mg kg <sup>-1</sup> ; approximately 30 % remaining after elimination	(Chen et al., 2014)
Fullerene (C <sub>60</sub> )	162 nm (t = 0 d), 215 nm (t = 9 d)	Water stirring	HPLC-MS	Waterborne exposure	1.0 µg L <sup>-1</sup>	21 d	Gastropod mollusc	<i>Radix</i> sp.	BCF: 17.9 (dry mass)	Quantitative A much higher value was observed for the degradation product (2670 L kg <sup>-1</sup> dw)	(Sanchís et al., 2020)
Fullerene (C <sub>60</sub> )	NA	40 mg of C <sub>60</sub> fullerenes were added to 12 g of vermiculite	HPLC	Soil	1000 mg L <sup>-1</sup>	21 d	Legumes	<i>Glycine max L.</i>		Quantitative Fullerenes were detected in the roots (218 000 µg kg <sup>-1</sup> ) but were not detected in the shoots	(De La Torre-Roche et al., 2012)
Fullerene (C <sub>60</sub> )	n/a	Dissolved in toluene	<sup>14</sup> C labelling, HPLC	Spiked soils	0.25 mg kg <sup>-1</sup> to 300 mg kg <sup>-1</sup> (dry mass)	14 d uptake and 7 d elimination	Oligochaete	<i>Eisenia fetida</i>	BSAF: 0.42	Quantitative BSAF for low dose soil: 0.42, and for high dose soils: 0.065 to 0.13	(Li et al., 2010)
Fullerene (C <sub>60</sub> )	285 nm	Water stirring	TEM	Spiked sediment	50 mg kg <sup>-1</sup> (dry mass)	28 d and 6 h elimination	Oligochaete	<i>Lumbriculus variegatus</i>		Qualitative Agglomerates observed in the gut tract but not absorption into gut epithelial cells	(Pakarinen et al., 2011)
Fullerene (C <sub>60</sub> )	208 nm or 179 nm with or without humic acid, respectively	Toluene-water exchange method	UV/vis spectroscopy, TEM	Algae ( <i>Scenedesmus obliquus</i> ) or algal after subcellular fractionation	15 mg kg <sup>-1</sup> to 65 mg kg <sup>-1</sup>	96 h uptake and 36 h elimination	Planktonic crustacean	<i>Daphnia magna</i>		Quantitative Uptake after 48 h was approximately 600 mg kg <sup>-1</sup> and 414 mg kg <sup>-1</sup> in without or with humic acid, respectively	(Chen et al., 2016)
Fullerene (C <sub>60</sub> )	280 nm to 420 nm	Ultrasonication	UV/vis spectroscopy, TEM, light microscopy	Clean tap water	1 mg L <sup>-1</sup> to 10 mg L <sup>-1</sup>	72 h	Planktonic crustacean	<i>Daphnia magna</i>		Quantitative Maximum body burden 614 mg kg <sup>-1</sup> wet mass; particles observed attached to gut tissue; after 72 h elimination, body burden decreased from 413 mg kg <sup>-1</sup> to 172 mg kg <sup>-1</sup>	(Lv et al., 2017)
Fullerene (C <sub>60</sub> )	139 ± 10 nm (DLS). 57.6 ± 26.1 nm (TEM)	Solvent exchange method with toluene and ethanol	UV/vis spectroscopy, light microscopy	Artificial freshwater with and without humic acid	0.2 mg L <sup>-1</sup> , 2 mg L <sup>-1</sup>	48 h uptake and 24 h elimination	Planktonic crustacean	<i>Daphnia magna</i>		Quantitative Model maximum body burden: 2268 mg kg <sup>-1</sup> ; approximately 20 %	(Chen et al., 2014)

(continued on next page)

Table 4 (continued)

Type	Average Size	Dispersion method	Detection method	Exposure	Concentration	Maximum Duration	Taxon	Species	Factor	Results	Reference
Fullerene (C <sub>60</sub> )	10 nm to 200 nm	Water stirring (with sunlight)	UV/vis spectroscopy	Waterborne exposure	30 mg L <sup>-1</sup>	4 d	Planktonic crustacean	<i>Daphnia magna</i>		remaining after elimination Quantitative Maximum body burden: 2 mg kg <sup>-1</sup>	(Oberdörster et al., 2006)
Fullerene (C <sub>60</sub> )	99 nm	Water exchange from tetrahydrofuran	UV/vis spectroscopy	Waterborne exposure	0.2 mg L <sup>-1</sup>	48 h	Planktonic crustacean	<i>Daphnia magna</i>	BCF: 437 500 (dry mass)	Quantitative BCF: 15 000 and 437 500 for mother and baby daphnia, respectively	(Tao et al., 2009)
Fullerene (C <sub>60</sub> )	235 nm	Water stirring	UV/vis spectroscopy, TEM, light microscopy	Artificial freshwater	0.5 mg L <sup>-1</sup> , 2 mg L <sup>-1</sup>	24 h uptake and 48 h elimination	Planktonic crustacean	<i>Daphnia magna</i>	BCF: 95 000 (dry mass)	Quantitative 24 % remained after 48 h elimination	(Tervonen et al., 2010)
Fullerene (C <sub>60</sub> )	210 nm to 1520 nm	Water stirring followed by sonication	TEM	Waterborne exposure	40 mg L <sup>-1</sup>	24 h	Planktonic crustacean	<i>Daphnia magna</i>		Qualitative Agglomerates observed in midgut lumen and epithelial cells	(Seke et al., 2017)
Fullerene (C <sub>60</sub> )	210 nm to 280 nm	Sonication in water	Light microscopy	Aerated tap water	0.1 mg L <sup>-1</sup> , 1 mg L <sup>-1</sup>	21 d	Planktonic crustacean	<i>Daphnia magna</i>		Qualitative Accumulated in gut tract	(Wang et al., 2019)
Fullerene (C <sub>60</sub> )	500 nm	Water stirring	LC-MS	MHW	3 mg L <sup>-1</sup> , 6 mg L <sup>-1</sup>	1 h	Planktonic crustacean	<i>Thamnocephalus platyurus</i>		Quantitative Observed in gut tract; no absorption into the gut epithelial cells was detected; maximum body burden of 6.8 µg/mg wet mass	(Patra et al., 2011)
Fullerene (C <sub>60</sub> )	NA	40 mg of C <sub>60</sub> fullerenes were added to 12 g of vermiculite	HPLC	Soil	1000 mg L <sup>-1</sup>	19 d	Rosid	<i>Cucurbita pepo L.</i>		Quantitative Fullerenes were detected in the roots (33.7 mg kg <sup>-1</sup> ), and in the shoots (61 µg kg <sup>-1</sup> to 4.49 mg kg <sup>-1</sup> (dry weight))	(De La Torre-Roche et al., 2012)
Fullerene (C <sub>70</sub> )	n/a	Probe sonication	Light microscopy, TEM, FTIR	Rice germination buffer	20 mg L <sup>-1</sup> , 800 mg L <sup>-1</sup>	9 d	Monocot (rice)	<i>Oryza sativa</i>		Qualitative Uptake was observed to occur simultaneously with the uptake of water and nutrients	(Lin et al., 2009)
Fullerenols	174.6 nm	Sonicated in water	<sup>13</sup> C labeling, IRMS, TEM	Aqueous exposure	1 mg L <sup>-1</sup>	36 h	Algae	<i>Scenedesmus obliquus</i>	BCF: 2170	Quantitative Particles observed inside the cells	(Shi et al., 2020b)
Fullerenols	200 nm to 300 nm (TEM)	Sonicated in water	<sup>13</sup> C labeling, TEM	Water exposure or fed algae	0.1 mg L <sup>-1</sup> , 1 mg L <sup>-1</sup>	24 h	Algae	<i>Scenedesmus obliquus</i>		Quantitative Maximum body burden: 1.95 g kg <sup>-1</sup> dry mass; uptake into cells observed	(Wang et al., 2018)
Fullerenols	174.6 nm	Sonicated in water	<sup>13</sup> C labeling	Feeding with <i>D. magna</i>	0.01 g wet weight of <i>D. magna</i> per fish daily (fullerene concentration was 6.93 g kg <sup>-1</sup> dry weight)	28 d uptake and 15 d elimination	Fish	<i>Danio rerio</i>	BMF: 0.54	Quantitative Half-life for elimination is 10.35 d; mainly located in intestine and liver but also detectable in gills, brains, and muscle	(Shi et al., 2020b)
Fullerenols	264.0 nm	Sonicated in water	<sup>13</sup> C labeling, TEM	Feeding with <i>D. magna</i>	0.01 g wet weight of <i>D. magna</i> per fish daily (fullerene concentration was	28 d uptake and 15 d elimination	Fish	<i>Danio rerio</i>	TTF: 0.49	Quantitative TTF for different tissues ranged from 0.26 to 0.49; highest concentrations	(Shi et al., 2020c)

(continued on next page)

Table 4 (continued)

Type	Average Size	Dispersion method	Detection method	Exposure	Concentration	Maximum Duration	Taxon	Species	Factor	Results	Reference
Fullerenols	50 nm to 200 nm	Unclear	MALDI-TOF-MS	Waterborne exposure	10 mg L <sup>-1</sup>	15 d	Fish	<i>Danio rerio</i>		were observed in the intestine and liver but also in the gill, muscle and brain; 60 % elimination within 3 d	(Shi et al., 2020a)
Fullerenols	264.0 nm	Sonicated in water	<sup>13</sup> C labeling, TEM	Artificial freshwater	2.5 mg L <sup>-1</sup>	72 h	Fish	<i>Daphnia magna</i>		Qualitative Fullerenol detected in the intestinal wall and all other tissues analyzed (brain, gills, intestines, muscle)	(Shi et al., 2020c)
Fullerenols	95 nm	Sonicated in water	<sup>13</sup> C labeling, SEM	Aqueous exposure	2.5 mg L <sup>-1</sup> to 10 mg L <sup>-1</sup>	7 d	Monocot (wheat)	<i>Triticum aestivum</i> L.		Quantitative Concentrations in roots were much higher than those in shoots and leaves	(Wang et al., 2016a)
Fullerenols	30 nm to 200 nm	Sonicated in water	<sup>13</sup> C labeling, TEM, light microscopy	Waterborne exposure	0.1 mg L <sup>-1</sup> , 1.0 mg L <sup>-1</sup>	48 h uptake and 48 h elimination	Planktonic crustacean	<i>Daphnia magna</i>	BCF: 5.51 × 10 <sup>6</sup>	Maximum body burden 13.66 g kg <sup>-1</sup> dry mass; excreted up to 97 %; accumulated fullerenols in gravid <i>D. magna</i> was transferred to the next generation of neonates	(Du et al., 2016)
Fullerenols	200 nm to 300 nm (TEM)	Sonicated in water	<sup>13</sup> C labeling, TEM	Water exposure or fed algae	0.1 mg L <sup>-1</sup> , 1 mg L <sup>-1</sup> (aqueous exposure) or algal exposure (unclear concentration)	24 h	Planktonic crustacean	<i>Daphnia magna</i>	BMF: 0.20; BAF: 39	Quantitative Maximum modeled BAF (aqueous exposure): 39; maximum modeled BAF (feeding exposure) 17	(Wang et al., 2018)
Fullerenols	174.6 nm	Sonicated in water	<sup>13</sup> C labeling	Feeding with algae	1 × 10 <sup>8</sup> cells L <sup>-1</sup> (fullerenol concentration unclear 2.17 mg g <sup>-1</sup> dry mass)	48 h	Planktonic crustacean	<i>Daphnia magna</i>	BMF: 3.20 (without elimination)	Quantitative Body burden: 6.93 g kg <sup>-1</sup> dry mass	(Shi et al., 2020b)

Abbreviations: bioconcentration factor (BCF), biomagnification factor (BMF), biota-soil accumulation factor (BSAF), dynamic light scattering (DLS), Fourier transform infrared spectroscopy (FTIR), high performance liquid chromatography (HPLC), isotope ratio mass spectrometry (IRMS), liquid chromatography-mass spectrometry (LC-MS), matrix assisted laser desorption/ionization-time of flight-mass spectrometry (MALDI-TOF-MS), scanning electron microscopy (SEM), transmission electron microscopy (TEM), trophic transfer factor (TTF), ultraviolet/visible (UV/vis).

**Table 5**  
Summary of nanoplastic bioaccumulation results.

Type (shape)	Average Size	Detection method	Exposure	Concentration	Maximum Duration	Taxon	Species	Factor	Results	Reference
Polyacrylonitrile with palladium doping, polystyrene shell (core-shell particle with a raspberry-shaped shell)	227.6 nm	ICP-MS	Dutch Standard Water (DSW)	0 % to 3 % plastic in sediment dw	28 d	Amphipod	<i>Gammarus pulex</i>		Quantitative Bioaccumulation of NPs positively correlated with NP concentration in sediment	(Redondo-Hasselerharm et al., 2021)
Polystyrene (sphere)	390 nm	SEM	F/2 medium	0 µg L <sup>-1</sup> to 5000 µg L <sup>-1</sup>	48 h	Algae	<i>Tisochrysis lutea</i>		Qualitative Particles adsorbed onto surface of microalgae at all concentrations; lower adsorption at lower concentrations	(Lebordais et al., 2021)
Polystyrene (sphere)	50 nm, 100 nm, and 1000 nm	Fluorescence	Filtered seawater	10 mg L <sup>-1</sup>	24 h	Bivalve mollusc (marine)	<i>Mytilus galloprovincialis</i>		Quantitative All particles were observed in the gills, stomach, and muscle	(Sendra et al., 2020a)
Polystyrene (sphere)	200 nm, 1000 nm	Fluorescence	Distilled water	1 × 10 <sup>-12</sup> mol L <sup>-1</sup>	24 h	Bivalve mollusc (marine)	<i>Dreissena rostriformis bugensis</i>		Quantitative 1000 nm particles move through gills through ciliated grooves in similar pathway to food particles; all bead sizes found in digestive tract; beads concentrated in siphons	(Merzel et al., 2020)
Polystyrene (sphere)	24 nm, 250 nm	<sup>14</sup> C labeling	Seawater	15 µg L <sup>-1</sup>	6 h uptake and 48 d elimination	Bivalve mollusc (marine)	<i>Pecten maximus</i>		Quantitative 250 nm particles were only in intestine, while 24 nm particles were also in other tissues; complete elimination of 24 nm particles in 14 d while some 250 nm particles still detected after 48 d	(Al-Sid-Cheikh et al., 2018)
Polystyrene (sphere)	50 nm and 100 nm	Molecular rotor probe methodology	Aqueous media (hydra test media)	1.25 mg L <sup>-1</sup> to 80 mg L <sup>-1</sup>	96 h	Cnidarian	<i>Hydra attenuata</i>		Quantitative Hydra internalized 100-nm NPs > 50 nm NPs; a fraction of the NPs were still present after 24 h elimination	(Auclair et al., 2020)
Polystyrene (sphere)	100 nm	Fluorescence	Artificial substitute ocean water	5 mg L <sup>-1</sup> to 50 mg L <sup>-1</sup>	72 h	Diatom	<i>Phaeodactylum tricorutum</i>		Quantitative Attachment onto the surface and potential internalization observed	(Sendra et al., 2019)
Polystyrene (sphere)	20 nm	TEM, fluorescence	Microinjection	1 % solid particle injection content, 0.027% nanoplastic in yolk sac	120 h	Fish	<i>Danio rerio</i>		Qualitative Bioaccumulation detected in brain	(Sökmen et al., 2020)
Polystyrene (sphere)	25 nm	Fluorescence	Aerated egg water	10 mg L <sup>-1</sup> to 100 mg L <sup>-1</sup>	120 h	Fish	<i>Danio rerio</i>		Qualitative Accumulation of PS in intestine, pancreas, gall bladder	(Brun et al., 2019)
Polystyrene (sphere)	100 nm	Fluorescence	De-chlorinated tap water	1 µg L <sup>-1</sup> to 100 µg L <sup>-1</sup>	14 d	Fish	<i>Oreochromis niloticus</i>		Quantitative Higher accumulation in gut and gills; lower accumulation in liver and brain	(Ding et al., 2018)
Polystyrene (sphere)	50 nm, 200 nm, 500 nm	Fluorescence	Aqueous medium (egg water and distilled water)	0.1 mg L <sup>-1</sup>	24 h	Fish	<i>Danio rerio</i>		Quantitative Highest fluorescence intensity observed in embryos for 50 nm particles; 50 nm particles were	(Lee et al., 2019)

(continued on next page)

Table 5 (continued)

Type (shape)	Average Size	Detection method	Exposure	Concentration	Maximum Duration	Taxon	Species	Factor	Results	Reference
Polystyrene (sphere)	50 nm, 1000 nm	Fluorescence	Dulbecco's modified Eagle's medium (DMEM) with 10 % fetal bovine serum (cells)	10 mg L <sup>-1</sup>	24 h (cells); 5 d (fish)	Fish	<i>Danio rerio</i> (ZF4 cells and whole fish)		observed throughout eggs while larger particles were mostly on chorion Quantitative 50 nm particles were internalized by cells > 1000 nm particles; uptake observed most clearly in the gut with detection in the skin, caudal fin and eyes for the 50 nm particles	(Sendra et al., 2021)
Polystyrene (sphere)	100 nm	Fluorescence	Dechlorinated carbon-filtered water	10 ug L <sup>-1</sup>	28 d	Fish	<i>Danio rerio</i>		Quantitative Particles detected in adult zebra and in the next generation	(Zhou et al. 2021)
Polystyrene (sphere)	25 nm, 50 nm, 250 nm, 700 nm	Fluorescence	Egg water with purchased stock	60 µg mL <sup>-1</sup>	48 h	Fish	<i>Danio rerio</i>		Qualitative Main uptake pathway through oral route compared to chorion and dermal uptake; 25 nm and 50 nm particles found in eye	(van Pomeroy et al., 2017)
Polystyrene (sphere)	700 nm	Fluorescence	Injection	5 mg mL <sup>-1</sup>	5 d	Fish	<i>Danio rerio</i>		Qualitative Some particle migration to heart and bloodstream	(Veneman et al., 2017)
Polystyrene (sphere)	25 nm to 330 nm	Hyperspectral imaging	Trophic transfer via <i>Daphnia magna</i>	0.005 g L <sup>-1</sup> to 0.150 g L <sup>-1</sup>	67 d	Fish	<i>Carassius carassius</i>		Quantitative Nanoparticles accumulated in brains	(Mattsson et al., 2017)
Polystyrene (sphere)	42 nm	Fluorescence	Added to fish food	10 % (by mass of fish food)	7 d	Fish	<i>Danio rerio</i>		Qualitative Parental transfer to embryos and larvae observed with detection in the liver, pancreas, yolk sack and GI tract	(Pitt et al., 2018)
Polystyrene (sphere)	50 nm	Fluorescence	Artificial freshwater	1 mg L <sup>-1</sup>	72 h	Fish	<i>Danio rerio</i>		Quantitative Bioaccumulation observed in zebrafish larvae	(Chen et al., 2017b)
Polystyrene (sphere)	5 nm	Fluorescence	Filtered natural seawater	10 mg L <sup>-1</sup>	2 h	Mysid crustacean	<i>Neomysis japonica</i>		Qualitative PS detected in stomach tissue	(Wang et al., 2020)
Polystyrene (sphere)	100 nm	Fluorescence	K media	1 ug L <sup>-1</sup> to 10,000 ug L <sup>-1</sup>	4.5 d	Nematode	<i>Caenorhabditis elegans</i>		Quantitative Particles detected in the intestine and gonads; some trophic transfer was observed	(Zhao et al. 2017a)
Polystyrene (sphere)	30 nm	Fluorescence	Aqueous media (naturally dechlorinated water)	34 ug L <sup>-1</sup>	48 h	Odonate insect	<i>Aphylla williamsoni</i>	BAF: 134,260	Quantitative Bioaccumulation observed	(Guimaraes et al., 2021)
Polystyrene (sphere)	200 nm	Light microscopy	Artificial freshwater	150 mg L <sup>-1</sup> , 250 mg L <sup>-1</sup>	24 h	Planktonic crustacean	<i>Thamnocephalus platyurus</i>		Qualitative Dose-dependent accumulation in the gut tract	(Saavedra et al., 2019)
Polystyrene (sphere)	25 nm	Fluorescence	Aqueous media (Elendt M4 media)	6.48 × 10 <sup>10</sup> particles mL <sup>-1</sup>	3 d	Planktonic crustacean	<i>Daphnia magna</i>		Qualitative NPs not observed to cross intestinal epithelium or in lipid droplets surrounding the gut after 2 d exposure; NPs located in fat droplets of embryos in brood pouch	(Brun et al., 2017)
Polystyrene (sphere)	200 nm	Light microscopy	Artificial freshwater	50 mg L <sup>-1</sup> , 100 mg L <sup>-1</sup>	48 h	Planktonic crustacean	<i>Daphnia magna</i>		Qualitative Dose-dependent accumulation in the gut tract	(Saavedra et al., 2019)

(continued on next page)

Table 5 (continued)

Type (shape)	Average Size	Detection method	Exposure	Concentration	Maximum Duration	Taxon	Species	Factor	Results	Reference
Polystyrene (sphere)	50 nm, 500 nm	Light microscopy	M4 medium	2.5% w/v (weight by volume)	48 h	Planktonic crustacean	<i>Daphnia magna</i>		Qualitative Accumulation of 50 nm particles on surface of thoracopods	(Ma et al., 2016)
Polystyrene (sphere)	568 nm	Fluorescence (after digestion procedure)	Artificial seawater	0.4 mg L <sup>-1</sup>	96 h	Polychaete	<i>Perinereis aibuhitensis</i>	BCF: 2	Quantitative Bioaccumulation observed	(Jiang et al., 2019)
Polystyrene (sphere)	200 nm	Fluorescence, TEM	Half-strength Murashige and Skoog (MS) basal medium	50 mg L <sup>-1</sup> (fluorescence), 100 mg L <sup>-1</sup> (TEM)	7d	Rosid	<i>Arabidopsis thaliana</i>		Qualitative Negatively charged particles were observed on the root tip and in the stele of the maturation zone; positively charged particles were mainly on the root hair with little in the root tissue; dialysis performed prior to testing	(Sun et al., 2020)
Polystyrene (sphere)	200 nm	Light microscopy	Artificial freshwater	50 mg L <sup>-1</sup> , 150 mg L <sup>-1</sup>	24 h	Rotifer	<i>Brachionus calyciflorus</i>		Qualitative Dose-dependent accumulation in the stomach	(Saavedra et al., 2019)
Polystyrene (sphere)	100 nm	Raman spectroscopy, SEM	Filtered natural seawater	4.55 × 10 <sup>8</sup> particles mL <sup>-1</sup> to 4.55 × 10 <sup>11</sup> particles mL <sup>-1</sup>	2 h	Tunicate (marine)	<i>Ciona Robusta</i>		Quantitative Low retention of PS particles; higher retention at lower particle concentration	(Valesia et al., 2021)
Polystyrene (sphere)	100 nm	Fluorescence	Artificial substitute ocean water (with and without feeding)	0.006 mg L <sup>-1</sup> , 0.6 mg L <sup>-1</sup>	24 h uptake and 24 h elimination	Zooplanktonic crustacean	<i>Artemia franciscana</i>		Quantitative A high fraction of the particles was ingested (60 % to 90 %)	(Sendra et al., 2020b)
Polystyrene and polycarbonate (round spherule agglomerates)	41 nm PS, 159 nm PC	Fluorescence	Filtered tap water	100 mg L <sup>-1</sup> plasma	1 h	Fish	<i>Pimephales promelas</i>		Qualitative Neutrophil phagocytosis of larger polystyrene nanoparticle agglomerates	(Greven et al., 2016)
Terephthalate (randomly-shaped pieced and agglomerates)	20 nm, 80 nm, 800 nm	Fluorescence	Aqueous medium (medium unclear)	10 mg L <sup>-1</sup>	168 h	Fish	<i>Danio rerio</i>		Quantitative Control groups with free dye showed limited uptake; uptake occurred in a size-dependent manner with 20 nm being the highest; particles observed in the yolk and on the chorion	(Ji et al., 2020)

Abbreviations: bioaccumulation factor (BAF), polycarbonate (PC), polystyrene (PS), scanning electron microscopy (SEM), transmission electron microscopy (TEM), bioconcentration factor (BCF), biomagnification factor (BMF), biota-soil accumulation factor (BSAF), dynamic light scattering (DLS), Fourier transform infrared spectroscopy (FTIR), high performance liquid chromatography (HPLC), isotope ratio mass spectrometry (IRMS), liquid chromatography-mass spectrometry (LC-MS), matrix assisted laser desorption/ionization-time of flight-mass spectrometry (MALDI-TOF-MS), trophic transfer factor (TTF), ultraviolet/visible (UV/vis).

compiled studies; Table 1). The use of  $^{14}\text{C}$  labeling has many advantages in that low detection limits can often be measured and definitive identification of the CNTs in complex matrices can be achieved as long as the  $^{14}\text{C}$  marker remains associated with the nanomaterial (Petersen et al., 2016). However, this approach does have disadvantages such as the cost, special synthesis required, safety concerns, and that its use is limited to laboratory studies (Petersen et al., 2016). It is also important to verify that all of the  $^{14}\text{C}$  label is associated with the CNT and not potential carbonaceous impurities such as amorphous carbon or hydrophobic organic contaminants that may have been formed during the CNT synthesis process or during suspension of the sample using ultrasonication (Petersen et al., 2016). The potential for the  $^{14}\text{C}$  label to be associated with hydrophobic organic contaminants can be assessed by performing leaching procedures with the particles and then testing for radioactivity by filtering a suspension and assessing if radioactivity is associated with the filtrate (Guo et al., 2013). Assessing whether the  $^{14}\text{C}$  label is associated with amorphous carbon is more challenging but can be evaluated by assessing non- $^{14}\text{C}$  labeled CNTs synthesized using the same process and evaluating the abundance of amorphous carbon (Petersen et al., 2008a,b).

Raman spectroscopy has also been extensively used in CNT bioaccumulation studies (24 % of the compiled studies). This approach can detect the unique spectral features of CNTs and identify them in complex matrices such as organism tissues (Edgington et al., 2014; Zhu et al., 2018) or nanocomposites (Piao et al., 2021). It is a promising orthogonal approach to confirm the presence of CNTs in organisms but is generally not used quantitatively. Another challenge with this technique is that it is sensitive to agglomerates versus individually dispersed CNTs which hinders assembly of calibration curves by adding varying CNT mass fractions to a specific matrix. Extraction of the CNTs prior to quantification may also induce changes to the CNT structure that can impact their Raman signal and therefore is typically not performed.

Two additional techniques that have been used in many CNT quantification studies are NIRF and the microwave method. NIRF has a low detection limit (62  $\mu\text{g}/\text{kg}$ ) but it can only detect individually dispersed semi-conducting SWCNTs and not bundles or metallic SWCNTs (Petersen et al., 2016). The microwave method is another promising technique for CNT bioaccumulation studies, but it uses a custom-built instrument that has only been used in a limited number of laboratories (Cano et al., 2016,2018; He et al., 2017).

### 3.2. Graphene family nanomaterials

Similar to CNTs, the most commonly used techniques in bioaccumulation studies of GFNs are  $^{14}\text{C}$  labeling, Raman spectroscopy, and EM (Tables 1 and 3). These techniques have similar strengths and limitations for GFNs as described above for CNTs (Goodwin et al., 2018). Briefly, the strengths and limitations for detection of  $^{14}\text{C}$ -labeled GFNs are the same as those for CNTs, because this technique is independent of what molecule or nanomaterial is labeled as long as the label remains associated (Guo et al., 2013). However, it is important to assess interferences, such as self-quenching, using LSC by comparing the radioactivity of compounds after direct addition to liquid scintillation media compared to combustion using a biological oxidizer and then LSC; lower values after direct addition to LSC cocktail suggest an interference (Goodwin et al., 2018; Guo et al., 2013). Raman spectroscopy can be used to investigate the same spectral features as when used with CNTs (e.g., the D and G bands) (Goodwin et al., 2018). Electron microscopy analysis has similar issues as with CNTs of identifying a CNM in a carbon matrix, and therefore, confirmatory techniques such as HRTEM and SAED should be used (Lu et al., 2017).

### 3.3. Fullerenes

The most commonly used techniques in bioaccumulation studies with fullerenes are TEM, light microscopy, and UV/vis spectroscopy

(Table 1). The challenges related to the use of TEM are similar to those for CNTs and GFNs, namely identifying a carbonaceous material in a carbon matrix (Waissi-Leinonen et al., 2012). Light microscopy is primarily used to identify the presence or absence of particles in the gut tract or attached to organism surfaces (Lin et al., 2009; Moore et al., 2019; Wang et al., 2019) and is thus typically used qualitatively.

In fullerene bioaccumulation experiments with relatively small organisms such as *D. magna*, UV/vis spectroscopy is often used to quantify the extracted fullerenes (Oberdörster et al., 2006; Tervonen et al., 2010). However, this approach only works when there is a sufficiently small amount of interfering material after the extraction process (Isaacson et al., 2009). When larger organisms are evaluated, mass spectrometry can be used to distinguish the fullerenes from interfering cellular material released during the extraction process (Isaacson et al., 2009; Wang et al., 2011). Using mass spectrometry has advantages over UV/vis spectroscopy such as more definitive quantitative analysis including the analysis of fragments (Reipa et al., 2018), quantitative analysis of different types of fullerenes, and more accurate analysis in the presence of interferences (Wang et al., 2010).

### 3.4. Nanoplastics

The most common method for analyzing nanoplastics is using fluorescently-labeled particles (72 % of studies; Table 1). However, there may be artifacts when using this method since some of the fluorescent label may not be associated with the particles (Catarino et al., 2019; Petersen et al., 2022a; Schür et al., 2019). An unsuccessful attempt to reproduce earlier published results on the uptake of plastic particles by *D. magna* was likely a result of the fluorescent probe leaching from the particles (Schür et al., 2019). Thus, studies with fluorescent probes sorbed to particles should be interpreted with caution since changes in the pH and ionic strength that can occur within the organism gut tract may lead to probe desorption in addition to the potential for desorption in the test media (Catarino et al., 2019). If the probe is attached to the particle through covalent bonding, the likelihood of release is much lower (Catarino et al., 2019). One promising technique for determining if the probe fluorescent molecule remains attached to the plastic particle is time-correlated single photon counting fluorescence lifetime imaging; this technique has recently been used with nanocellulose particles (Patel et al., 2021) and should be investigated for usage in nanoplastic bioaccumulation studies.

Several other techniques have been recently developed and used in a limited number of studies (Blanco et al., 2021; Mitrano et al., 2019; Redondo-Hasselerharm et al., 2021; Valsesia et al., 2021). For example, using nanoplastic particles with a metal core could enable analysis by single particle inductively coupled plasma-mass spectrometry (spICP-MS) or ICP-MS contingent upon metal ions not being released by the particles during the course of the study (Mitrano et al., 2019; Redondo-Hasselerharm et al., 2021). This technique is similar to using  $^{14}\text{C}$  labeled particles, an approach that has also been successfully used in a nanoplastic bioaccumulation study (Al-Sid-Cheikh et al., 2018), in that both labeling techniques are not applicable to field studies. In addition, pyrolysis gas chromatography/mass spectrometry (pyrGC/MS) was used to identify nanoplastics in water with natural organic matter (NOM) and algal cells (Blanco et al., 2021). Additional work to evaluate the use of this method in organism tissues after digestion and extraction would be valuable.

## 4. Bioaccumulation results

### 4.1. Exposure concentration

The selected exposure concentration can be influenced by many factors such as environmental relevance, the detection limit(s) of the analytical technique(s), and adherence to standardized methods with a specified test concentration. Thus, it is unsurprising that they vary

broadly among the different studies. The exposure concentration would typically not be expected to impact some bioaccumulation results (e.g., bioaccumulation factors) because the concentration in the organism is normalized by the exposure concentration. However, it would impact the body burden, which is not normalized, with higher body burdens expected at higher exposure concentrations. One difference between testing dissolved chemicals and CNMs or nanoplastics is that higher particle concentrations could lead to increased particle sizes through homoagglomeration and potentially also increased settling (Su et al., 2017). If homoagglomeration occurs, the organism would be exposed to different sized agglomerates depending upon the exposure concentration, which could influence uptake and absorption across epithelial surfaces.

#### 4.2. Exposure methods

All of the different bioaccumulation studies were assessed to determine what exposure conditions were used (Table S1). Overall, most studies were performed with aqueous exposures instead of using soil or sediment. The particles most frequently tested in soil or sediment were fullerenes and fullereneols (29 % of studies), while there was only a single sediment bioaccumulation study (3 %) with nanoplastics. In addition, most studies were conducted without feeding exposure (80 % to 90 % of studies). Testing particle uptake with feeding exposure is more complex because the analytical method needs to be able to detect the carbonaceous particle in this matrix. In addition, measurements may be needed to confirm that the particles are associated with the food source and not freely suspended in the test media to distinguish between uptake from freely available particles and those associated with food (Mortimer et al., 2016a,2016b). Density gradient centrifugation may be needed to separate cells or small organisms (e.g., *Caenorhabditis elegans*) and suspended particles (Johnson et al., 2021,2017; Mortimer et al., 2016a,2016b).

#### 4.3. Carbon nanotubes

Forty-two qualitative and quantitative CNT bioaccumulation studies (Bisesi et al., 2015,2014; Cano et al., 2016; Chen et al., 2015; Edgington et al., 2014; Ferguson et al., 2008; Galloway et al., 2010; Ghafari et al., 2008; Gogos et al., 2016; Hanna et al., 2014; Kennedy et al., 2008; Lahiani et al., 2013; Lahiani et al., 2016; Larue et al., 2012; Leeuw et al., 2007; Li and Huang 2011; Li et al., 2013; Lin et al., 2009; Liu et al., 2009; Maes et al., 2014; Martinez-Ballesta et al., 2016; Mortimer et al., 2016b; Mouchet et al., 2011,2010,2008,2007; Mwangi et al., 2012; Parks et al., 2014,2013; Petersen et al., 2009,2008a,b,2010,2011a,2011b; Rhiem et al., 2015; Roberts et al., 2007; Schierz et al., 2014; Smirnova et al., 2012; Smith et al., 2007; Wang et al., 2016b; Yang et al., 2011; Zhai et al., 2015; Zhu et al., 2006) were reported in a previous publication (Bjorkland et al., 2017). While plant uptake of CNTs was often observed (Khodakovskaya et al., 2011; Larue et al., 2012; Zhai et al., 2015), 13 quantitative bioaccumulation studies (Bisesi et al., 2015; Bisesi et al., 2014; Ferguson et al., 2008; Leeuw et al., 2007; Li et al., 2013; Maes et al., 2014; Mortimer et al., 2016b; Parks et al., 2013; Petersen et al., 2008a,b,2010,2011b; Schierz et al., 2014) in a wide range of multicellular organisms other than plants showed low absorption across epithelial surfaces and low persistence in the organism. In many studies, the concentration measured could be attributed to soil or sediment present in the gut tract (Li et al., 2013; Petersen et al., 2008a,b,2010,2011b). In a study with fruit flies (*Drosophila melanogaster*), absorption across the gut tract was observed, but the concentration outside of the gut tract was only  $10^{-8}$  of the total dose (Leeuw et al., 2007). Studies using fish did not detect CNTs outside of the gut tract using NIRF (Bisesi et al., 2015,2014), while a study using  $^{14}\text{C}$  labeled multiwall CNTs (MWCNTs) did detect low concentrations: 0.07 % and 0.04 % of the body burden in the blood and fillet, respectively, after exposure for 168 h. Biomagnification was also not observed in three quantitative

studies (Mortimer et al., 2016b; Parks et al., 2013; Schierz et al., 2014). Studies that performed qualitative measurements, such as with TEM or Raman spectroscopy, of absorption across epithelial surfaces in multicellular organisms other than plants also did not observe uptake (Edgington et al., 2014; Mouchet et al., 2011,2010,2008,2007). In aggregate, these results led to the overall conclusion that bioaccumulation of CNTs in multicellular organisms other than plants was likely to be low.

In this study, eight new CNT bioaccumulation studies were identified (Cano et al., 2018; Cano et al., 2017; Hennig et al., 2019; Politowski et al., 2021; Soubaneh et al., 2020; Zhao et al., 2017b; Zhu et al., 2018,2017), covering a broad range of organisms including plants, zooplankton, fish, and oligochaetes (Table 2). Similar to some earlier studies on plant uptake of various types of CNTs (Khodakovskaya et al., 2011; Larue et al., 2012; Zhai et al., 2015), three additional studies reported uptake into plant food crops and leaves under hydroponic exposure conditions (McGehee et al., 2017; Zhao et al., 2017b) and after addition to soils (Cano et al., 2016). Similar to two previous studies with oligochaete *Lumbriculus variegatus* (Petersen et al., 2008b,2010), an additional study with oligochaete *L. variegatus* exposed to raw MWCNTs and MWCNTs released from a polymer nanocomposite after aging, biota sediment accumulation factors were less than 1 (Hennig et al., 2019). This result indicated that the concentration in the organism was less than that in the sediment, a finding similar to previous bioaccumulation studies with *L. variegatus* (Petersen et al., 2008b,2010). *D. magna* were shown to ingest large quantities of CNTs leading to high body burden values (Cano et al., 2017). Trophic transfer of MWCNTs was observed from *D. magna* to fathead minnows (Cano et al., 2018). However, the limited number of fish tested ( $n = 5$  fish for each treatment), the high standard errors ( $\approx 30$  % or greater), and the low concentration of MWCNTs in the *D. magna* (close to the detection limit), hinder drawing firm conclusions about the biomagnification trends. In addition, the fish did not have their gut tract voided and thus it was not possible to distinguish between CNTs in the gut tract and those absorbed into other tissues. Since previous studies have shown a lack of CNT distribution in fish (Bisesi et al., 2015,2014; Maes et al., 2014), it is probable that the CNTs in this study were held within the gut lumen of one organism and transferred to the gut lumen of the higher trophic level without absorption or tissue bioaccumulation.

However, one recent study showed radioactively-labeled ethanolamine-functionalized CNTs present in the head bone canals of a fish species (*Salvelinus alpinus*) after aqueous exposure to a CNT dispersion, suggesting that absorption and distribution throughout the fish body had occurred, with accumulation primarily occurring in the head (Soubaneh et al., 2020). It is unclear if these differing results, compared to three other fish bioaccumulation studies that did not detect CNTs in fish brains after exposure (Bisesi et al., 2015,2014; Maes et al., 2014), could stem from the different CNT coatings used. In addition, the CNTs were detected using autoradiography of the radioactive probe. The presence of CNTs in the head tissues was not directly confirmed using an orthogonal method (e.g., TEM); the concentration of CNTs in these tissues was not quantified; and a mechanistic explanation for these results was not provided. Control experiments conducted with the radioactive ethanolamine coating to evaluate its bioaccumulation showed a different distribution within the organism which suggests that these results do not stem from uptake of the freely available  $^{14}\text{C}$  label. Another possible explanation is that the  $^{14}\text{C}$  label associated with impurities present in the CNTs (e.g., catalyst impurities or amorphous carbon), which then were absorbed into the fish.

#### 4.4. Fullerenes

Twenty-seven studies were found on the bioaccumulation of fullerenes or fullereneols by different organisms (Table 3). Uptake of fullerenes and fullereneols into the shoots and leaves was observed in exposed plants in hydroponic studies (Avanasi et al., 2014; Lin et al., 2009; Wang et al., 2016a) and also in studies with vermiculite (De La Torre-Roche

et al., 2012) or sand (Avanasi et al., 2014). This finding is similar to studies with CNTs (Cano et al., 2016; Khodakovskaya et al., 2011; Larue et al., 2012; Zhai et al., 2015).

Most fullerene uptake studies were performed using *D. magna*. In some studies, several percent of the total organism mass was fullerenes (Tervonen et al., 2010). A wide range of different *D. magna* ages and exposure conditions were tested (Chen et al., 2014; Pakarinen et al., 2013), hindering comparison among studies. It is probable that the organism size impacted the body burden values, at least in the absence of gut voiding, with larger organisms having smaller body burden values since the gut tract is a smaller fraction of the total organism size (Petersen et al., 2019b).

Trophic transfer of fullerenols was evaluated from algae to *D. magna* and from *D. magna* to zebrafish (Shi et al., 2020b,2020c). In the study evaluating trophic transfer from algae to *D. magna*, trophic transfer was observed for fullerenols (biomagnification factor (BMF) value of 3.2) and 59 % of the fullerenols associated with algae were transferred to *D. magna* in the presence of humic acid (Shi et al., 2020b). However, studies evaluating trophic transfer of fullerenols from *D. magna* to zebrafish did not show trophic transfer (BMF < 1) (Shi et al., 2020b,2020c). One explanation for this finding is that the fullerenols associated with the *D. magna* may have been largely in the organism's digestive tract, which would indicate a lack of trophic transfer even for BMF values >1. Nevertheless, the zebrafish did show apparent absorption of fullerenols across the gut tract and into different tissues such as the brain and liver (Shi et al., 2020a; Shi et al., 2020b; Shi et al., 2020c).

The findings related to the absorption of fullerenols across the zebrafish gut tract largely differ from the findings of fish studies with CNTs and of FLG, which showed limited absorption (Bisesi et al., 2015; Bisesi et al., 2014; Lu et al., 2017; Maes et al., 2014). However, one study with small FLG particles (lateral diameter of 20–70 nm and a thickness of 1 nm) did show absorption into the liver through the intestines (Lu et al., 2017). There are several potential explanations for the fullereneol findings. These authors measured the fullerenols in these tissues with either isotope-ratio mass spectrometry (IRMS) measuring <sup>13</sup>C labeled particles, matrix-assisted laser desorption/ionization (MALDI), or TEM. However, the TEM measurements performed did not conclusively confirm the particle identity using HRTEM, SAED, or EELS. It is important to note that the authors did sonicate the fullerenols to suspend them. This process may have caused fragmentation of these particles, resulting in smaller particles or molecules that could then be absorbed by the organisms; while fragmentation of fullerenols after ultrasonication has not been evaluated to our knowledge, this process was shown to degrade CNTs (Heller et al., 2005), which would likely be more chemically stable than fullerenols. Particle fragments would not be distinguished from intact particles using IRMS, and as stated above, TEM analysis did not conclusively confirm the particle identity. While the suspension was characterized using dynamic light scattering (DLS), this technique is known to potentially miss smaller particles (Petersen et al., 2019a) because the sensitivity is proportional to the diameter to the sixth power (Stetefeld et al., 2016).

It may be that individual fullereneol particles or small agglomerates were suspended, and that these small particles had different uptake patterns than larger CNT and FLG particles. Interestingly, a study using <sup>14</sup>C labeled fullerenes in a toluene suspension added to soils (Li et al., 2010) did find higher bioaccumulation factor (BAF) values by earthworms than studies using FLG, SWCNTs, or MWCNTs (Mao et al., 2016; Petersen et al., 2008a,b,2010). This may be due to the presence of individual fullerene particles given their ability to be individually suspended in toluene (Pycke et al., 2011) and due to their smaller size compared to larger fullerene agglomerates that could lead to higher uptake. The BAF values measured for some conditions in this study (Li et al., 2010) were beyond the range that could be explained by soil remaining in the organism gut tract after the gut voidance process (prior to bioaccumulation measurements, earthworms are typically allowed to eliminate approximately 95 % of the soil in the gut tract). This suggests

that individual fullerene, and likely also fullereneol, particles may have different bioaccumulation behaviors than larger CNMs, agglomerated CNMs, and nanoplastics.

#### 4.5. Graphene

Sixteen studies were identified that evaluated the bioaccumulation of GFNs using 11 different species and 9 different taxa (Table 4). The bioaccumulation results differed among the taxa tested. For the plant species, there was GFN uptake measured using <sup>13</sup>C or <sup>14</sup>C labeling into the roots for all plants (rice, wheat, and peas) (Chen et al., 2017a; Chen et al., 2019; Huang et al., 2018). Uptake into the roots and leaves was observed for rice (Huang et al., 2018) and peas (Chen et al., 2019), but not for wheat-exposed to GO (Chen et al., 2017a). Single-celled species had high bioconcentration factor (BCF) values such as 126,000 for *Tetrahymena thermophile* (Dong et al., 2018). Within the same study (Dong et al., 2018), substantially smaller BCF factors were calculated for *D. magna* (7783) and *Danio rerio* ( $\approx 32$ ), indicating lower bioaccumulation with increasing organism size. High body burdens were observed for some multicellular organisms such as *D. magna* (e.g., 7.8 mg kg<sup>-1</sup>), but elimination was often fairly quick (within 24 h to 48 h), especially in the presence of algae (Guo et al., 2013).

Trophic transfer among single-celled species (*T. thermophila* fed *Escherichia coli* that had bioaccumulated FLG) showed biomagnification with a maximum BMF of 8.57 (Dong et al., 2018). At higher trophic levels there was a decrease in the graphene concentration indicated by BMF values below 1: maximum BMFs of 0.013 and 0.014 were observed for *D. magna* that were fed *T. thermophila* and for *D. rerio* that were fed *D. magna*, respectively (Dong et al., 2018). These results suggest an overall lack of biomagnification for multicellular species although biomagnification may occur among single-celled species (e.g., bacteria to protozoa).

Detectable concentrations of FLG passed across the digestive tract for some organisms such as for *D. rerio* (Lu et al., 2017) and the mollusc *Cipangopaludina cathayensis* (Su et al., 2018b) where FLGs were detected in the liver. In both studies, the presence of the FLG was quantified using <sup>14</sup>C labeling, while the presence of FLG in the hepatocytes was confirmed using HRTEM and Raman spectroscopy. Nevertheless, the FLG concentrations observed in the livers of *D. rerio* and *C. cathayensis* were only 1.1 % (Lu et al., 2017) and 1.3 % (Su et al., 2018b), respectively, of the total body burden.

#### 4.6. Nanoplastics

Thirty different laboratory studies have evaluated the bioaccumulation of nanoplastics using a wide range of organisms (Table 5). While there is a broad range of plastic products in commerce, >90 % of these studies evaluated uptake of PS particles. It appears that the prevalence in use of PS in these studies is because of the availability of fluorescently-labelled nanoplastic PS particles from commercial suppliers (e.g., (Catarino et al., 2019)), and developed methods to prepare <sup>14</sup>C-labeled PS (e.g., (Al-Sid-Cheikh et al., 2020)) or inorganic metal (e.g., Pd) labeled PS particles (e.g., (Redondo-Hasselerharm et al., 2021)). Analysis of nanoplastics in biological tissues to confirm absorption and quantify accumulation has required detection of these labels by various methods, each with their own limitations. In one study that used hyperspectral imaging and suggested that nanoplastic particles had been transferred to fish brains, relevant control data were not included to conclusively identify the particles such as the spectra of the particles by themselves, or of the particles after being directly added to fish brains (Mattsson et al., 2017). In addition, an orthogonal approach was not used to confirm the results.

Seventy-two percent of nanoplastic bioaccumulation studies used fluorescently labeled particles, which as described earlier, may have significant issues with artifacts if the fluorescent probe is released from the particles (Blanco et al., 2021; Petersen et al., 2022a; Valsesia et al.,

2021). However, some studies have performed control experiments to assess bioaccumulation of the probe by itself (e.g., Ji et al., 2020) or dialyzed the particles prior to the experiments to remove the free probe (e.g., Sun et al., 2020). In studies that evaluated nanoplastic bioaccumulation using fluorescence, many observe absorption across epithelial surfaces using fluorescent labeling (e.g., Ding et al., 2018; Ji et al., 2020; Sendra et al., 2020a), but a robust orthogonal method was typically not used to confirm the result. Given the lack of orthogonal measurements (e.g., HRTEM) and the necessary control experiments, it is challenging to draw firm conclusions from these studies. Furthermore, the frequent observance of absorption across epithelial surfaces contrasts with studies performed using other CNMs which typically are not absorbed (Bisesi et al., 2015; Bisesi et al., 2014; Ferguson et al., 2008; Leeuw et al., 2007; Li et al., 2013; Lu et al., 2017; Maes et al., 2014; Mortimer et al., 2016b; Parks et al., 2013; Petersen et al., 2008a,b,2010; Petersen et al., 2011b; Schierz et al., 2014; Su et al., 2018b).

Nevertheless, absorption of nanoplastics across epithelial surfaces has also been observed in studies using alternative approaches. In one study, preparation of  $^{14}\text{C}$ -labeled PS particles (Al-Sid-Cheikh et al., 2020) has enabled detection of particles in soft tissues after digestion process and via autoradiography in the scallop *Pecten maximus* (Al-Sid-Cheikh et al., 2018). While the method of  $^{14}\text{C}$  labeled PS indicated translocation across epithelial membranes in *P. maximus*, the best evidence of translocation appears to be the presence of the nanoplastics within the adductor muscles of the scallops. Within the adductor muscle, the particles appear uniformly distributed throughout the tissue at low concentrations and agglomerated together as accumulations consistent with the size of haemocytes (10–30  $\mu\text{m}$  diameter). It was suggested in this paper (Al-Sid-Cheikh et al., 2018) that the labeled nanoplastics became associated with haemocytes when haemocytes were located on external tissues surfaces and subsequently brought into the interior of the adductor muscle by these cells rather than by direct absorption of the particles across tissue membranes. In addition, a sediment-exposure study using metal-doped particles observed that approximately 1 % of the nanoplastics absorbed by amphipod *Gammarus pulex* were located in a body compartment from which depuration was minimal after 28 d (Redondo-Hasselerharm et al., 2021). It was unclear if this fraction was adsorbed to an epithelial surface such as microvilli or was absorbed across an epithelial surface.

## 5. Discussion

For all of the engineered CNMs described in this study, there were no bioaccumulation results from field studies, in part because the expected concentration of fullerenes, CNTs, and GFNs in organism tissues would be below the detection limits of available analytical techniques (Goodwin et al., 2018; Petersen et al., 2016). In a bioaccumulation screening framework developed during a Pellston workshop, the greatest weight of evidence was placed on food web biomagnification derived from field data (Gobas et al., 2009). Unlike the information available for many chemicals from field studies, the assessment of bioaccumulation potential for engineered CNMs is limited to laboratory studies. In contrast, there are a multitude of field studies measuring microplastics in organisms. In these studies, >99 % of all particles, identified using a range of methods, were located in the organisms' gut tract (Gouin 2020). As a result of a lack of robust analytical methods for quantifying nanoplastics in field organisms, there are not yet studies on this topic, but work is ongoing (Blanco et al., 2021).

Extremely high bioaccumulation metrics (e.g., BCF values) have been observed for many of the CNMs and nanoplastics described in this study with particles accounting for several percent of the organism dry mass (including particles contained in gut tracts that had not been voided) (Petersen et al., 2009). However, these values differ from those observed for dissolved hydrophobic organic chemicals that have ready passage across the gut tract: most quantitative studies of engineered CNMs have shown limited absorption (e.g., approximately 1 % or less of

the body burden in fish (Bisesi et al., 2015; Bisesi et al., 2014; Lu et al., 2017; Maes et al., 2014)) across the gut tract of multicellular organisms other than plants (Bisesi et al., 2015; Bisesi et al., 2014; Ferguson et al., 2008; Leeuw et al., 2007; Li et al., 2013; Lu et al., 2017; Maes et al., 2014; Mortimer et al., 2016b; Parks et al., 2013; Petersen et al., 2008a,b,2010; Petersen et al., 2011b; Schierz et al., 2014; Su et al., 2018b); there are some studies that have shown different results, but methodological issues hinder understanding if those results stem from testing different types of particles (e.g., fullerenols) (Shi et al., 2020a; Shi et al., 2020b; Shi et al., 2020c) or CNTs with different surface coatings (Soubaneh et al., 2020). This suggests that the BAF values observed for CNMs and nanoplastics may not be directly comparable to those for other types of contaminants that are readily absorbed across the gut tract and transported throughout the organism, and should be interpreted differently.

In addition to studies on uptake by a single organism, it is also important to assess whether CNMs and nanoplastics can be biomagnified at higher trophic levels. Overall, trophic transfer studies suggest a lack of biomagnification among multi-cellular organisms. While biomagnification factor values >1 (indicative of trophic transfer) have been observed for transfer among single-celled organisms (e.g., bacteria to protozoa) in one study (Dong et al., 2018) but not in another (Mortimer et al., 2016b), biomagnification factors have consistently been less than 1 for larger organisms (e.g., *D. magna* and *D. rerio*) (Dong et al., 2018) except for studies with fullerenols (Shi et al., 2020b; Shi et al., 2020c). This suggests that, while trophic transfer may occur, it is unlikely that significant absorption across the gut tract will occur in higher trophic level organisms.

Gaining a definitive understanding of the bioaccumulation potential of CNMs and nanoplastics requires better analytical methods, especially for nanoplastics. Many of the nanoplastic studies rely solely upon fluorescent labeling which has been demonstrated to be vulnerable to artifacts from probe molecules separated from particles (Catarino et al., 2019; Petersen et al., 2022b; Schür et al., 2019). Several recent studies have focused on method development for quantifying nanoplastics in tissues or cells, and more work is needed on this topic (Blanco et al., 2021; Valsesia et al., 2021). However, all methods have potential limitations, and many studies have revealed potential artifacts. Therefore, careful experimental design is needed to rule out alternative hypotheses (e.g., that a probe is separated from the CNM or nanoplastic) when performing bioaccumulation studies. This is critical when the results show absorption across epithelial surfaces by CNMs or nanoplastics, which has typically not been observed. Orthogonal measurements are essential to confirm results obtained. Additional analytical method development and careful bioaccumulation studies are needed to improve clarity about the potential for carbon nanomaterials to be biodistributed throughout organism tissues and the ecological risks these particles may pose a return.

### Supporting Information

Definitions for bioaccumulation terms used throughout this manuscript and a table summarizing an evaluation of exposure conditions in CNM and nanoplastic bioaccumulation studies.

### Declaration of Competing Interest

The authors declare that they have no known competing financial interests or personal relationships that could have appeared to influence the work reported in this paper.

### Acknowledgements

This work was supported in part by the Natural Environment Research Council, UK, grant no. NERC/NE/N006526/1.

## Appendix A. Supplementary material

Supplementary data to this article can be found online at <https://doi.org/10.1016/j.envint.2022.107650>.

## References

- Al-Sid-Cheikh, M., Rowland, S.J., Stevenson, K., Rouleau, C., Henry, T.B., Thompson, R. C., 2018. Uptake, whole-body distribution, and depuration of nanoplastics by the scallop pecten maximus at environmentally realistic concentrations. *Environ. Sci. Tech.* 52, 14480–14486.
- Al-Sid-Cheikh, M., Rowland, S.J., Kaegi, R., Henry, T.B., Cormier, M.-A., Thompson, R.C., 2020. Synthesis of <sup>14</sup>C-labelled polystyrene nanoplastics for environmental studies. *Commun. Mater.* 1, 97.
- ASTM (American Society for Testing Materials) International, 2006. E2456-06: standard terminology relating to nanotechnology. West Conshohocken, PA.
- Auclair, J., Quinn, B., Peyrot, C., Wilkinson, K.J., Gagne, F., 2020. Detection, biophysical effects, and toxicity of polystyrene nanoparticles to the cnidarian *Hydra attenuata*. *Environ. Sci. Pollut. Res.* 27, 11772–11781.
- Avanasi, R., Jackson, W.A., Sherwin, B., Mudge, J.F., Anderson, T.A., 2014. C60 fullerene soil sorption, biodegradation, and plant uptake. *Environ. Sci. Tech.* 48, 2792–2797.
- Bisesi, J.H., Merten, J., Liu, K., Parks, A.N., Afroz, A., Glenn, J.B., Klaine, S.J., Kane, A. S., Saleh, N.B., Ferguson, P.L., Sabo-Attwood, T., 2014. Tracking and quantification of single-walled carbon nanotubes in fish using near infrared fluorescence. *Environ. Sci. Tech.* 48, 1973–1983.
- Bisesi Jr., J.H., Thuy, N., Ponnawolu, S., Liu, K., Lavelle, C.M., Afroz, A.R.M.N., Saleh, N. B., Ferguson, P.L., Denslow, N.D., Sabo-Attwood, T., 2015. Examination of single-walled carbon nanotubes uptake and toxicity from dietary exposure: tracking movement and impacts in the gastrointestinal system. *Nanomaterials* 5, 1066–1086.
- Bjorkland, R., Tobias, D.A., Petersen, E.J., 2017. Increasing evidence indicates low bioaccumulation of carbon nanotubes. *Environ. Sci. Nano* 4, 747–766.
- Blanchon, F., Davranche, M., El Hadri, H., Grassl, G., Gigault, J., 2021. Nanoplastics identification in complex environmental matrices: strategies for polystyrene and polypropylene. *Environ. Sci. Tech.* 55, 8753–8759.
- Brun, N.R., Beenakker, M.M.T., Hunting, E.R., Ebert, D., Vijver, M.G., 2017. Brood pouch-mediated polystyrene nanoparticle uptake during *Daphnia magna* embryogenesis. *Nanotoxicology* 11, 1059–1069.
- Brun, N.R., van Hage, P., Hunting, E.R., Haramis, A.-P.-G., Vink, S.C., Vijver, M.G., Schaaf, M.J.M., Tudorache, C., 2019. Polystyrene nanoplastics disrupt glucose metabolism and cortisol levels with a possible link to behavioural changes in larval zebrafish. *Commun. Biol.* 2, 382.
- Burschka, J., Pellet, N., Moon, S.J., Humphry-Baker, R., Gao, P., Nazeeruddin, M.K., Gratzel, M., 2013. Sequential deposition as a route to high-performance perovskite-sensitized solar cells. *Nature* 499, 316.
- Cano, A.M., Kohl, K., Deleon, S., Payton, P., Irin, F., Saed, M., Shah, S.A., Green, M.J., Canas-Carrell, J.E., 2016. Determination of uptake, accumulation, and stress effects in corn (*Zea mays* L.) grown in single-wall carbon nanotube contaminated soil. *Chemosphere* 152, 117–122.
- Cano, A.M., Maul, J.D., Saed, M., Shah, S.A., Green, M.J., Canas-Carrell, J.E., 2017. Bioaccumulation, stress, and swimming impairment in *Daphnia magna* exposed to multiwalled carbon nanotubes, graphene, and graphene oxide. *Environ. Toxicol. Chem.* 36, 2199–2204.
- Cano, A.M., Maul, J.D., Saed, M., Irin, F., Shah, S.A., Green, M.J., French, A.D., Klein, D. M., Crago, J., Canas-Carrell, J.E., 2018. Trophic transfer and accumulation of multiwalled carbon nanotubes in the presence of copper ions in *daphnia magna* and fathead minnow (*pimephales promelas*). *Environ. Sci. Tech.* 52, 794–800.
- Catarino, A.I., Frutos, A., Henry, T.B., 2019. Use of fluorescent-labelled nanoplastics (NPs) to demonstrate NP absorption is inconclusive without adequate controls. *Sci. Tot. Environ.* 670, 915–920.
- Chen, Q., Yin, D., Li, J., Hu, X., 2014. The effects of humic acid on the uptake and depuration of fullerene aqueous suspensions in two aquatic organisms. *Environ. Toxicol. Chem.* 33, 1090–1097.
- Chen, Q., Hu, X., Yin, D., Wang, R., 2016. Effect of subcellular distribution on nC<sub>60</sub> uptake and transfer efficiency from *Scenedesmus obliquus* to *Daphnia magna*. *Ecotoxicol. Environ. Saf.* 128, 213–221.
- Chen, Q., Gundlach, M., Yang, S., Jiang, J., Velki, M., Yin, D., Hollert, H., 2017b. Quantitative investigation of the mechanisms of microplastics and nanoplastics toward zebrafish larvae locomotor activity. *Sci. Tot. Environ.* 584–585, 1022–1031.
- Chen, G.S., Qiu, J.L., Liu, Y., Jiang, R.F., Cai, S.Y., Liu, Y., Zhu, F., Zeng, F., Luan, T.G., Ouyang, G.F., 2015. Carbon nanotubes act as contaminant carriers and translocate within plants. *Sci. Rep.* 5.
- Chen, L., Wang, C., Li, H., Qu, X., Yang, S.-T., Chang, X.-L., 2017a. Bioaccumulation and Toxicity of C-13-skeleton labeled graphene oxide in wheat. *Environ. Sci. Tech.* 51, 10146–10153.
- Chen, L., Wang, C., Yang, S., Guan, X., Zhang, Q., Shi, M., Yang, S.-T., Chen, C., Chang, X.-L., 2019. Chemical reduction of graphene enhances in vivo translocation and photosynthetic inhibition in pea plants. *Environ. Sci. Nano* 6, 1077–1088.
- De La Torre-Roche, R., Hawthorne, J., Deng, Y.Q., Xing, B.S., Cai, W.J., Newman, L.A., Wang, C., Ma, X.M., White, J.C., 2012. Fullerene-enhanced accumulation of p,p'-DDE in agricultural crop species. *Environ. Sci. Tech.* 46, 9315–9323.
- Ding, J., Zhang, S., Razanajatovo, R.M., Zou, H., Zhu, W., 2018. Accumulation, tissue distribution, and biochemical effects of polystyrene microplastics in the freshwater fish red tilapia (*Oreochromis niloticus*). *Environ. Pollut.* 238, 1–9.
- Dong, S., Xia, T., Yang, Y., Lin, S., Mao, L., 2018. Bioaccumulation of C-14-labeled graphene in an aquatic food chain through direct uptake or trophic transfer. *Environ. Sci. Tech.* 52, 541–549.
- Du, M.M., Zhang, H., Li, J.X., Yan, C.Z., Zhang, X., Chang, X.L., 2016. Bioaccumulation, depuration, and transfer to offspring of c-13-labeled fullerene by *daphnia magna*. *Environ. Sci. Tech.* 50, 10421–10427.
- Edgington, A.J., Petersen, E.J., Herzog, A.A., Podila, R., Rao, A., Klaine, S.J., 2014. Microscopic investigation of single-wall carbon nanotube uptake by *Daphnia magna*. *Nanotoxicology* 8, 2–10.
- Elliott, J.T., Rosslein, M., Song, N.W., Toman, B., Kinsner-Ovaskainen, A., Maniratanachote, R., Salit, M.L., Petersen, E.J., Sequeira, F., Romsos, E.L., Kim, S.J., Lee, J., von Moos, N.R., Rossi, F., Hirsch, C., Krug, H.F., Suchaoin, W., Wick, P., 2017. Toward achieving harmonization in a nanocytotoxicity assay measurement through an interlaboratory comparison study. *Altex-Alt. Anim. Exper.* 34, 201–218.
- Fan, W., Liu, Y., Xu, Z., Wang, X., Li, X., Luo, S., 2016. The mechanism of chronic toxicity to *Daphnia magna* induced by graphene suspended in a water column. *Environ. Sci. Nano* 3, 1405–1415.
- Feng, Y.P., Lu, K., Mao, L., Guo, X.K., Gao, S.X., Petersen, E.J., 2015. Degradation of C-14-labeled few layer graphene via Fenton reaction: Reaction rates, characterization of reaction products, and potential ecological effects. *Water Res.* 84, 49–57.
- Ferguson, P.L., Chandler, G.T., Templeton, R.C., Demarco, A., Scrivens, W.A., Englehart, B.A., 2008. Influence of sediment-amendment with single-walled carbon nanotubes and diesel soot on bioaccumulation of hydrophobic organic contaminants by benthic invertebrates. *Environ. Sci. Tech.* 42, 3879–3885.
- Galloway, T., Lewis, C., Dolciotti, I., Johnston, B.D., Moger, J., Regoli, F., 2010. Sublethal toxicity of nano-titanium dioxide and carbon nanotubes in a sediment dwelling marine polychaete. *Environ. Pollut.* 158, 1748–1755.
- Ghafari, P., St-Denis, C.H., Power, M.E., Jin, X., Tsou, V., Mandal, H.S., Bols, N.C., Tang, X.W., 2008. Impact of carbon nanotubes on the ingestion and digestion of bacteria by ciliated protozoa. *Nat. Nanotech.* 3, 347–351.
- Gobas, F.A., de Wolf, W., Burkhard, L.P., Verbruggen, E., Plotzke, K., 2009. Revisiting bioaccumulation criteria for POPs and PBT assessments. *Integ. Environ. Ass. Manag.* 5, 624–637.
- Gogos, A., Moll, J., Klingenfuss, F., van der Heijden, M., Irin, F., Green, M.J., Zenobi, R., Bucheli, T.D., 2016. Vertical transport and plant uptake of nanoparticles in a soil mesocosm experiment. *J. Nanobiotechnol.* 14.
- Goodwin, D.G., Adeleye, A.S., Sung, L., Ho, K.T., Burgess, R.M., Petersen, E.J., 2018. Detection and quantification of graphene-family nanomaterials in the environment. *Environ. Sci. Tech.* 52, 4491–4513.
- Gouin, T., 2020. Toward an improved understanding of the ingestion and trophic transfer of microplastic particles: critical review and implications for future research. *Environ. Toxicol. Chem.* 39, 1119–1137.
- Greven, A.-C., Merk, T., Karagöz, F., Mohr, K., Klapper, M., Jovanović, B., Palić, D., 2016. Polycarbonate and polystyrene nanoplastic particles act as stressors to the innate immune system of fathead minnow (*Pimephales promelas*). *Environ. Toxicol. Chem.* 35, 3093–3100.
- Guimaraes, A.T.B., Rodrigues, A.S.D., Pereira, P.S., Silva, F.G., Malafaia, G., 2021. Toxicity of polystyrene nanoplastics in dragonfly larvae: an insight on how these pollutants can affect benthic macroinvertebrates. *Sci. Tot. Environ.* 752.
- Guo, X., Dong, S., Petersen, E.J., Gao, S., Huang, Q., Mao, L., 2013. Biological uptake and depuration of radio-labeled graphene by *daphnia magna*. *Environ. Sci. Tech.* 47, 12524–12531.
- Halamoda, B., Baccannier, S., Bastogne, T., Bazile, D., Boisseau, P., Borchard, G., Borgos, S.E., Calzolari, L., Cederbrant, K., Felice, G., Di Francesco, T., Dobrovolskaia, M., Gaspar, R., Gracia, B., Hackley, V., Leyens, L., Liptrott, N., Park, M., Patri, A., Bremer, S., 2019. Bridging communities in the field of nanomedicine. *Regul. Toxicol. Pharm.* 106.
- Hanna, S.K., Miller, R.J., Lenihan, H.S., 2014. Deposition of carbon nanotubes by a marine suspension feeder revealed by chemical and isotopic tracers. *J. Hazard. Mater.* 279, 32–37.
- Hanna, S.K., Cooksey, G.A., Dong, S., Nelson, B.C., Mao, L., Elliott, J.T., Petersen, E.J., 2016. Feasibility of using a standardized *Caenorhabditis elegans* toxicity test to assess nanomaterial toxicity. *Environ. Sci. Nano* 3, 1080–1089.
- Hanna, S.K., Montoro Bustos, A.R., Peterson, A.W., Reipa, V., Scanlan, L.D., Hosbas Coskun, S., Cho, T.J., Johnson, M.E., Hackley, V.A., Nelson, B.C., Winchester, M.R., Elliott, J.T., Petersen, E.J., 2018. Agglomeration of *escherichia coli* with positively charged nanoparticles can lead to artifacts in a standard *caenorhabditis elegans* toxicity assay. *Environ. Sci. Tech.* 52, 5968–5978.
- He, Y., Al-Abed, S.R., Dionysiou, D.D., 2017. Quantification of carbon nanotubes in different environmental matrices by a microwave induced heating method. *Sci. Tot. Environ.* 580, 509–517.
- Heller, D.A., Barone, P.W., Strano, M.S., 2005. Sonication-induced changes in chiral distribution: a complication in the use of single-walled carbon nanotube fluorescence for determining species distribution. *Carbon* 43, 651–653.
- Hennig, M.P., Maes, H.M., Ottermanns, R., Schaeffer, A., Siebers, N., 2019. Release of radiolabeled multi-walled carbon nanotubes (C-14-MWCNT) from epoxy nanocomposites into quartz sand-water systems and their uptake by *Lumbriculus variegatus*. *Nanoimpact* 14.
- Huang, C., Xia, T., Niu, J., Yang, Y., Lin, S., Wang, X., Yang, G., Mao, L., Xing, B., 2018. Transformation of C-14-labeled graphene to (CO<sub>2</sub>)-C-14 in the shoots of a rice plant. *Angew. Chem.-Int. Ed.* 57, 9759–9763.
- Isaacson, C.W., Kleber, M., Field, J.A., 2009. Quantitative analysis of fullerene nanomaterials in environmental systems: a critical review. *Environ. Sci. Tech.* 43, 6463–6474.
- ISO (International Organization for Standardization), 2010. TS 80004-1: nanotechnologies — vocabulary — Part 1: Core terms. Geneva, Switzerland.

- ISO, 2020. ISO/TR 21960:2020 Plastics — Environmental aspects — State of knowledge and methodologies.
- Ji, Y.X., Wang, C.Y., Wang, Y.Q., Fu, L.W., Man, M.S., Chen, L.X., 2020. Realistic polyethylene terephthalate nanoplastics and the size- and surface coating-dependent toxicological impacts on zebrafish embryos. *Environ. Sci. Nano* 7, 2313–2324.
- Jiang, X.T., Tian, L.L., Ma, Y.N., Ji, R., 2019. Quantifying the bioaccumulation of nanoplastics and PAHs in the clamworm *Perinereis aibuhitensis*. *Sci. Tot. Environ.* 655, 591–597.
- Johnson, M.E., Hanna, S.K., Bustos, A.R.M., Sims, C.M., Elliott, L.C.C., Lingayat, A., Johnston, A.C., Nikoobakht, B., Elliott, J.T., Holbrook, R.D., Scoto, K.C.K., Murphy, K.E., Petersen, E.J., Yu, L.L., Nelson, B.C., 2017. Separation, sizing, and quantitation of engineered nanoparticles in an organism model using inductively coupled plasma mass spectrometry and image analysis. *ACS Nano* 11, 526–540.
- Johnson, M.E., Bennett, J., Montoro Bustos, A.R., Hanna, S.K., Kolmakov, A., Sharp, N., Petersen, E.J., Lapasset, P.E., Sims, C.M., Murphy, K.E., Nelson, B.C., 2021. Combining secondary ion mass spectrometry image depth profiling and single particle inductively coupled plasma mass spectrometry to investigate the uptake and biodistribution of gold nanoparticles in *Caenorhabditis elegans*. *Anal. Chem. Acta* 1175, 338671.
- Kennedy, A.J.H.M.S., Steevens, J.A., Dontsova, K.M., Chappell, M.A., Gunter, J.C., Weiss Jr., C.A., 2008. Factors influencing the partitioning and toxicity of nanotubes in the aquatic environment. *Environ. Toxicol. Chem.* 27, 1932–1941.
- Khodakovskaya, M.V., de Silva, K., Nedosekin, D.A., Dervishi, E., Biris, A.S., Shashkov, E. V., Galanzha, E.I., Zharov, V.P., 2011. Complex genetic, photothermal, and photoacoustic analysis of nanoparticle-plant interactions. *PNAS* 108, 1028–1033.
- Klaine, S.J., Alvarez, P.J.J., Batley, G.E., Fernandes, T.F., Handy, R.D., Lyon, D.Y., Mahendra, S., McLaughlin, M.J., Lead, J.R., 2008. Nanomaterials in the environment: Behavior, fate, bioavailability, and effects. *Environ. Toxicol. Chem.* 27, 1825–1851.
- Købler, C., Saber, A.T., Jacobsen, N.R., Wallin, H., Vogel, U., Qvortrup, K., Mølhave, K., 2014. FIB-SEM imaging of carbon nanotubes in mouse lung tissue. *Anal. Bioanal. Chem.* 406, 3863–3873.
- Lagier, L., Mouchet, F., Laplanche, C., Mottier, A., Cadarsi, S., Evariste, L., Sarrieu, C., Lonchambon, P., Pinelli, E., Flahaut, E., Gauthier, L., 2017. Surface area of carbon-based nanoplastics prevails on dispersion for growth inhibition in amphibians. *Carbon* 119, 72–81.
- Lahiani, M.H., Dervishi, E., Chen, J.H., Nima, Z., Gaume, A., Biris, A.S., Khodakovskaya, M.V., 2013. Impact of carbon nanotube exposure to seeds of valuable crops. *ACS Appl. Mater. Int.* 5, 7965–7973.
- Lahiani, M.H., Dervishi, E., Ivanov, I., Chen, J.H., Khodakovskaya, M., 2016. Comparative study of plant responses to carbon-based nanomaterials with different morphologies. *Nanotechnol.* 27.
- Larue, C., Pinaut, M., Czarny, B., Georgin, D., Jaillard, D., Bendiab, N., Mayne-L'Hermite, M., Taran, F., Dive, V., Carriere, M., 2012. Quantitative evaluation of multi-walled carbon nanotube uptake in wheat and rapeseed. *J. Hazard. Mater.* 227, 155–163.
- Lebordais, M., Gutierrez-Villagomez, J.M., Gigault, J., Baudrimont, M., Langlois, V.S., 2021. Molecular impacts of dietary exposure to nanoplastics combined with arsenic in Canadian oysters (*Crassostrea virginica*) and bioaccumulation comparison with Caribbean oysters (*Isognomon alatus*). *Chemosphere* 277, 130331.
- Lee, W.S., Cho, H.J., Kim, E., Huh, Y.H., Kim, H.J., Kim, B., Kang, T., Lee, J.S., Jeong, J., 2019. Bioaccumulation of polystyrene nanoplastics and their effect on the toxicity of Au ions in zebrafish embryos. *Nanoscale* 11, 3173–3185.
- Leeuw, T.K., Reith, R.M., Simonette, R.A., Harden, M.E., Cherukuri, P., Tsyboulski, D.A., Beckingham, K.M., Weisman, R.B., 2007. Single-walled carbon nanotubes in the intact organism: Near-IR imaging and biocompatibility studies in *Drosophila*. *Nano Lett.* 7, 2650–2654.
- Li, D., Fortner, J.D., Johnson, D.R., Chen, C., Li, Q.L., Alvarez, P.J.J., 2010. Bioaccumulation of  $^{14}\text{C}_{60}$  by the Earthworm *Eisenia fetida*. *Environ. Sci. Tech.* 44, 9170–9175.
- Li, M.H., Huang, C.P., 2011. The responses of *Ceriodaphnia dubia* toward multi-walled carbon nanotubes: effect of physical-chemical treatment. *Carbon* 49, 1672–1679.
- Li, S.B., Irin, F., Atore, F.O., Green, M.J., Canas-Carrell, J.E., 2013. Determination of multi-walled carbon nanotube bioaccumulation in earthworms measured by a microwave-based detection technique. *Sci Tot Environ* 445, 9–13.
- Lin, S.J., Reppert, J., Hu, Q., Hudson, J.S., Reid, M.L., Ratnikova, T.A., Rao, A.M., Luo, H., Ke, P.C., 2009. Uptake, translocation, and transmission of carbon nanomaterials in rice plants. *Small* 5, 1128–1132.
- Liu, X.Y., Vinson, D., Abt, D., Hurt, R.H., Rand, D.M., 2009. Differential toxicity of carbon nanomaterials in *Drosophila*: Larval dietary uptake is benign, but adult exposure causes locomotor impairment and mortality. *Environ. Sci. Tech.* 43, 6357–6363.
- Lu, K., Huang, Q., Wang, P., Mao, L., 2015. Physicochemical changes of few-layer graphene in peroxidase-catalyzed reactions: characterization and potential ecological effects. *Environ. Sci. Tech.* 49.
- Lu, K., Dong, S., Petersen, E.J., Niu, J., Chang, X., Wang, P., Lin, S., Gao, S., Mao, L., 2017. Biological uptake, distribution, and depuration of radio-labeled graphene in adult zebrafish: effects of graphene size and natural organic matter. *ACS Nano* 11, 2872–2885.
- Lv, X., Huang, B., Zhu, X., Jiang, Y., Chen, B., Tao, Y., Zhou, J., Cai, Z., 2017. Mechanisms underlying the acute toxicity of fullerene to *Daphnia magna*: energy acquisition restriction and oxidative stress. *Water Res.* 123, 696–703.
- Lv, X., Yang, Y., Tao, Y., Jiang, Y., Chen, B., Zhu, X., Cai, Z., Li, B., 2018. A mechanism study on toxicity of graphene oxide to *Daphnia magna*: direct link between bioaccumulation and oxidative stress. *Environ. Pollut.* 234, 953–959.
- Ma, Y., Huang, A., Cao, S., Sun, F., Wang, L., Guo, H., Ji, R., 2016. Effects of nanoplastics and microplastics on toxicity, bioaccumulation, and environmental fate of phenanthrene in fresh water. *Environ. Pollut.* 219, 166–173.
- Maes, H.M., Stibany, F., Giefers, S., Daniels, B., Deutschmann, B., Baumgartner, W., Schaffer, A., 2014. Accumulation and distribution of multiwalled carbon nanotubes in zebrafish (*danio rerio*). *Environ. Sci. Tech.* 48, 12256–12264.
- Mao, L., Liu, C., Lu, K., Su, Y., Gu, C., Huang, Q., Petersen, E.J., 2016. Exposure of few layer graphene to *Limnodrilus hoffmeisteri* modifies the graphene and changes its bioaccumulation by other organisms. *Carbon* 109, 566–574.
- Martinez-Ballesta, M.C., Zapata, L., Chalbi, N., Carvajal, M., 2016. Multiwalled carbon nanotubes enter broccoli cells enhancing growth and water uptake of plants exposed to salinity. *J. Nanobiotechnol.* 14.
- Mattsson, K., Johnson, E.V., Malmendal, A., Linse, S., Hansson, L.-A., Cedervall, T., 2017. Brain damage and behavioural disorders in fish induced by plastic nanoparticles delivered through the food chain. *Sci. Rep.* 7, 11452.
- McGehee, D.L., Lahiani, M.H., Irin, F., Green, M.J., Khodakovskaya, M.V., 2017. Multiwalled carbon nanotubes dramatically affect the fruit metabolome of exposed tomato plants. *ACS Appl. Mater. Int.* 9, 32430–32435.
- Merzel, R.L., Purser, L., Soucy, T.L., Olszewski, M., Colón-Bernal, I., Duhaime, M., Elgin, A.K., Banaszak Holl, M.M., 2020. Uptake and retention of nanoplastics in quagga mussels. *Global Challenge.* 4, 1800104.
- Mesarić, T., Gambardella, C., Milivojević, T., Faimali, M., Drobne, D., Falugi, C., Makovec, D., Jemec, A., Sepić, K., 2015. High surface adsorption properties of carbon-based nanomaterials are responsible for mortality, swimming inhibition, and biochemical responses in *Artemia salina* larvae. *Aquat. Toxicol.* 163, 121–129.
- Mitrano, D.M., Beltzung, A., Frehland, S., Schmiedgruber, M., Cingolani, A., Schmidt, F., 2019. Synthesis of metal-doped nanoplastics and their utility to investigate fate and behaviour in complex environmental systems. *Nat. Nanotech.* 14, 362–368.
- Moore, E.A., Babbitt, C.W., Connelly, S.J., Tyler, A.C., Rogalsky, G., 2019. Cascading ecological impacts of fullerenes in freshwater ecosystems. *Environ. Toxicol. Chem.* 38, 1714–1723.
- Mortimer, M., Petersen, E.J., Buchholz, B.A., Holden, P.A., 2016a. Separation of bacteria, protozoa and carbon nanotubes by density gradient centrifugation. *Nanomaterials* 6.
- Mortimer, M., Petersen, E.J., Buchholz, B.A., Orias, E., Holden, P.A., 2016b. Bioaccumulation of multiwall carbon nanotubes in tetrahymena thermophila by direct feeding or trophic transfer. *Environ. Sci. Tech.* 50, 8876–8885.
- Mortimer, M., Kefela, T., Trinh, A., Holden, P.A., 2021. Uptake and depuration of carbon and boron nitride-based nanomaterials in the protozoa *Tetrahymena thermophila*. *Environ. Sci. Nano* 8, 3613–3628.
- Mouchet, F.L., Flahaut, P., Pinelli, E., Gauthier, L., 2007. Assessment of the potential in vivo ecotoxicity of double-walled carbon nanotubes (DWNs) in water, using the amphibian *Ambystoma mexicanum*. *Nanotoxicology* 1, 149–156.
- Mouchet, F., Landois, P., Sarramejean, E., Bernard, G., Puech, P., Pinelli, E., Flahaut, E., Gauthier, L., 2008. Characterisation and in vivo ecotoxicity evaluation of double-walled carbon nanotubes in larvae of the amphibian *Xenopus laevis*. *Aquat. Toxicol.* 87, 127–137.
- Mouchet, F., Landois, P., Puech, P., Pinelli, E., Flahaut, E., Gauthier, L., 2010. Carbon nanotube ecotoxicity in amphibians: assessment of multiwalled carbon nanotubes and comparison with double-walled carbon nanotubes. *Nanomem. Nanotechnol. Biol. Med.* 5, 963–974.
- Mouchet, F., Landois, P., Datsyuk, V., Puech, P., Pinelli, E., Flahaut, E., Gauthier, L., 2011. International amphibian micronucleus standardized procedure (ISO 21427–1) for in vivo evaluation of double-walled carbon nanotubes toxicity and genotoxicity in water. *Environ. Toxicol.* 26, 136–145.
- Mwangi, J.N., Wang, N., Ingersoll, C.G., Hardesty, D.K., Brunson, E.L., Li, H., Deng, B.L., 2012. Toxicity of carbon nanotubes to freshwater aquatic invertebrates. *Environ. Toxicol. Chem.* 31, 1823–1830.
- Nguyen, B., Claveau-Mallet, D., Hernandez, L.M., Xu, E.G., Farmer, J.M., Tufenkji, N., 2019. Separation and analysis of microplastics and nanoplastics in complex environmental samples. *Acc. Chem. Res.* 52, 858–866.
- Oberdörster, E., Zhu, S.Q., Blickley, T.M., McClellan-Green, P., Haasch, M.L., 2006. Ecotoxicology of carbon-based engineered nanoparticles: Effects of fullerene ( $\text{C}_{60}$ ) on aquatic organisms. *Carbon* 44, 1112–1120.
- Pakarinen, K., Petersen, E.J., Leppänen, M.T., Akkanen, J., Kukkonen, J.V.K., 2011. Adverse effects of fullerenes ( $\text{nC}(60)$ ) spiked to sediments on *Lumbricus variegatus* (*Oligochaeta*). *Environ. Pollut.* 159, 3750–3756.
- Pakarinen, K., Petersen, E.J., Alvila, L., Waissi-Leinonen, G.C., Akkanen, J., Leppänen, M. T., Kukkonen, J.V.K., 2013. A screening study on the fate of fullerenes ( $\text{nC60}$ ) and their toxic implications in natural freshwaters. *Environ. Toxicol. Chem.* 32, 1224–1232.
- Parks, A.N., Portis, L.M., Schierz, P.A., Washburn, K.M., Perron, M.M., Burgess, R.M., Ho, K.T., Chandler, G.T., Ferguson, P.L., 2013. Bioaccumulation and toxicity of single-walled carbon nanotubes to benthic organisms at the base of the marine food chain. *Environ. Toxicol. Chem.* 32, 1270–1277.
- Parks, A.N., Burgess, R.M., Ho, K.T., Ferguson, P.L., 2014. On the likelihood of single-walled carbon nanotubes causing adverse marine ecological effects. *Integ Environ Ass Manag* 10, 472–474.
- Patel, I., Woodcock, J., Beams, R., Stranick, S.J., Nieuwendaal, R., Gilman, J.W., Mullen, M.R., Sayes, C.M., Salari, M., DeLoid, G., Demokritou, P., Harper, B., Harper, S., Ong, K.J., Shatkin, J.A., Fox, D.M., 2021. Fluorescently labeled cellulose nanofibers for environmental health and safety studies. *Nanomaterials* (Basel, Switzerland) 11, 1015.
- Patra, M., Ma, X., Isaacson, C., Bouchard, D., Poynton, H., Lazorchak, J.M., Rogers, K.R., 2011. Changes in agglomeration of fullerenes during ingestion and excretion in *Thamnocephalus platyurus*. *Environ. Toxicol. Chem.* 30, 828–835.

- Petersen, E.J., Barrios, A.C., Henry, T.B., Johnson, M.E., Koelmans, A.A., Montoro Bustos, A.R., Matheson, J., Roesslein, M., Zhao, J., Xing, B., 2022. Potential artifacts and control experiments in toxicity tests of nanoplastic and microplastic particles. *Environ. Sci. Technol.* (in press).
- Petersen, E.J., Huang, Q.G., Weber Jr., W.J., 2008a. Bioaccumulation of radio-labeled carbon nanotubes by *Eisenia foetida*. *Environ. Sci. Tech.* 42, 3090–3095.
- Petersen, E.J., Huang, Q.G., Weber Jr., W.J., 2008b. Ecological uptake and depuration of carbon nanotubes by *Lumbriculus variegatus*. *Environ. Health Perspect.* 116, 496–500.
- Petersen, E.J., Akkanen, J., Kukkonen, J.V.K., Weber Jr., W.J., 2009. Biological uptake and depuration of carbon nanotubes by *Daphnia magna*. *Environ. Sci. Tech.* 43, 2969–2975.
- Petersen, E.J., Huang, Q.G., Weber Jr., W.J., 2010. Relevance of octanol-water distribution measurements to the potential ecological uptake of multi-walled carbon nanotubes. *Environ. Toxicol. Chem.* 29, 1106–1112.
- Petersen, E.J., Pinto, R.A., Mai, D.J., Landrum, P.F., Weber Jr., W.J., 2011a. Influence of polyethyleneimine graftings of multi-walled carbon nanotubes on their accumulation and elimination by and toxicity to *Daphnia magna*. *Environ. Sci. Tech.* 45, 1133–1138.
- Petersen, E.J., Pinto, R.A., Zhang, L., Huang, Q.G., Landrum, P.F., Weber, W.J., 2011b. Effects of polyethyleneimine-mediated functionalization of multi-walled carbon nanotubes on earthworm bioaccumulation and sorption by soils. *Environ. Sci. Tech.* 45, 3718–3724.
- Petersen, E.J., Pinto, R.A., Shi, X.Y., Huang, Q.G., 2012. Impact of size and sorption on degradation of trichloroethylene and polychlorinated biphenyls by nano-scale zerovalent iron. *J. Hazard. Mater.* 243, 73–79.
- Petersen, E.J., Flores-Cervantes, D.X., Bucheli, T.D., Elliott, L.C.C., Fagan, J.A., Gogos, A., Hanna, S., Kägi, R., Mansfield, E., Bustos, A.R.M., Plata, D.L., Reipa, V., Westerhoff, P., Winchester, M.R., 2016. Quantification of carbon nanotubes in environmental matrices: current capabilities, case studies, and future prospects. *Environ. Sci. Tech.* 50, 4587–4605.
- Petersen, E.J., Bustos, A.R.M., Toman, B., Johnson, M.E., Ellefson, M., Caceres, G.C., Neuer, A.L., Chan, G., Kemling, J.W., Mader, B., Murphy, K., Roesslein, M., 2019a. Determining what really counts: modeling and measuring nanoparticle number concentrations. *Environ. Sci. Nano* 6, 2876–2896.
- Petersen, E.J., Mortimer, M., Burgess, R.M., Handy, R., Hanna, S., Ho, K.T., Johnson, M., Loureiro, S., Selck, H., Scott-Fordsmand, J.J., Spurgeon, D., Urine, J., van den Brink, N.W., Wang, Y., White, J., Holden, P., 2019b. Strategies for robust and accurate experimental approaches to quantify nanomaterial bioaccumulation across a broad range of organisms. *Environ. Sci. Nano* 6, 1619–1656.
- Petersen, E.J., Hirsch, C., Elliott, J.T., Krug, H.F., Aengenheister, L., Arif, A.T., Bogna, A., Kinsner-Ovaskainen, A., May, S., Walser, T., Wick, P., Roesslein, M., 2020. Cause-and-effect analysis as a tool to improve the reproducibility of nanobioassays: four case studies. *Chem. Res. Toxicol.* 33, 1039–1054.
- Petersen, E.J., Barrios, A.C., Henry, T.B., Johnson, M.E., Koelmans, A.A., Montoro Bustos, A.R., Matheson, J., Roesslein, M., Zhao, J., Xing, B., 2022. Potential artifacts and control experiments in toxicity tests of nanoplastic and microplastic particles. *Environ. Sci. Tech.*
- Piao, Y., Tondare, V.N., Davis, C.S., Gorham, J.M., Petersen, E.J., Gilman, J.W., Scott, K., Vladar, A.E., 2021. Hight Walker, A.R. Comparative study of multiwall carbon nanotube nanocomposites by Raman, SEM, and XPS measurement techniques. *Compos. Sci. Technol.* 208, 108753.
- Pitt, J.A., Trevisan, R., Massarsky, A., Kozal, J.S., Levin, E.D., Di Giulio, R.T., 2018. Maternal transfer of nanoplastics to offspring in zebrafish (*Danio rerio*): a case study with nanopolyethylene. *Sci. Tot. Environ.* 643, 324–334.
- Polittowski, I., Wittmers, F., Hennig, M.P., Siebers, N., Goffart, B., Roß-Nickoll, M., Ottermann, R., Schäffer, A., 2021. A trophic transfer study: accumulation of multi-walled carbon nanotubes associated to green algae in water flea *Daphnia magna*. *NanoImpact* 22, 100303.
- Praetorius, A., Tufenkji, N., Goss, K.U., Scheringer, M., von der Kammer, F., Elimelech, M., 2014. The road to nowhere: equilibrium partition coefficients for nanoparticles. *Environ. Sci. Nano* 1, 317–323.
- Pycke, B.F.G., Benn, T.M., Herckes, P., Westerhoff, P., Halden, R.U., 2011. Strategies for quantifying C-60 fullerene in environmental and biological samples and implications for studies in environmental health and ecotoxicology. *Trends Anal. Chem.* 30, 44–57.
- Pycke, B.F.G., Chao, T.C., Herckes, P., Westerhoff, P., Halden, R.U., 2012. Beyond nC (60): strategies for identification of transformation products of fullerene oxidation in aquatic and biological samples. *Anal. Bioanal. Chem.* 404, 2583–2595.
- Redondo-Hasselherm, P., Vink, G., Mitran, D.M., Koelmans, A.A., 2021. Metal-doping of nanoplastics enables accurate assessment of uptake and effects on *Gammarus pulex*. *Environ. Sci. Nano* 8, 1761–1770.
- Reipa, V., Hanna, S.K., Urbas, A., Sander, L., Elliott, J., Conny, J., Petersen, E.J., 2018. Efficient electrochemical degradation of multiwall carbon nanotubes. *J. Hazard. Mater.* 354, 275–282.
- Rhiem, S., Riding, M.J., Baumgartner, W., Martin, F.L., Semple, K.T., Jones, K.C., Schaffer, A., Maes, H.M., 2015. Interactions of multiwalled carbon nanotubes with algal cells: Quantification of association, visualization of uptake, and measurement of alterations in the composition of cells. *Environ. Pollut.* 196, 431–439.
- Roberts, A.P., Mount, A.S., Seda, B., Souther, J., Qiao, R., Lin, S., Ke, P., Rao, A.M., Klaine, S.J., 2007. In vivo biomodification of lipid-coated carbon nanotubes by *Daphnia magna*. *Environ. Sci. Tech.* 41, 3025–3029.
- Roesslein, M., Hirsch, C., Kaiser, J.P., Krug, H.F., Wick, P., 2013. Comparability of in vitro tests for bioactive nanoparticles: a common assay to detect reactive oxygen species as an example. *Int. J. Mol. Sci.* 14, 24320–24337.
- Saavedra, J., Stoll, S., Slaveykova, V.I., 2019. Influence of nanoplastic surface charge on eco-corona formation, aggregation and toxicity to freshwater zooplankton. *Environ. Pollut.* 252, 715–722.
- Sanchís, J., Llorca, M., Olmos, M., Schirinzi, G.F., Bosch-Orea, C., Abad, E., Barceló, D., Farré, M., 2018. Metabolic responses of *Mytilus galloprovincialis* to fullerenes in mesocosm exposure experiments. *Environ. Sci. Tech.* 52, 1002–1013.
- Sanchís, J., Freixa, A., López-Doval, J.C., Santos, L.H.M.L.M., Sabater, S., Barceló, D., Abad, E., Farré, M., 2020. Bioconcentration and bioaccumulation of C60 fullerene and C60 epoxide in biofilms and freshwater snails (*Radix* sp.). *Environ. Res.* 180, 108715.
- Schierz, A., Parks, A.N., Washburn, K.M., Chandler, G.T., Ferguson, P.L., 2012. Characterization and quantitative analysis of single-walled carbon nanotubes in the aquatic environment using near-infrared fluorescence spectroscopy. *Environ. Sci. Tech.* 46, 12262–12271.
- Schierz, A., Espinasse, B., Wiesner, M.R., Bisesi, J.H., Sabo-Attwood, T., Ferguson, P.L., 2014. Fate of single walled carbon nanotubes in wetland ecosystems. *Environ. Sci. Nano* 1, 574–583.
- Schür, C., Rist, S., Baun, A., Mayer, P., Hartmann, N.B., Wagner, M., 2019. When fluorescence is not a particle: the tissue translocation of microplastics in *daphnia magna* seems an artifact. *Environ. Toxicol. Chem.* 38, 1495–1503.
- Seke, M., Markelic, M., Morina, A., Jovic, D., Korac, A., Milicic, D., Djordjevic, A., 2017. Synergistic mitotoxicity of chloromethanes and fullerene C(60) nanoaggregates in *Daphnia magna* midgut epithelial cells. *Protoplasma* 254, 1607–1616.
- Sendra, M., Staffieri, E., Yeste, M.P., Moreno-Garrido, I., Gatica, J.M., Corsi, I., Blasco, J., 2019. Are the primary characteristics of polystyrene nanoplastics responsible for toxicity and ad/absorption in the marine diatom *Phaeodactylum tricornutum*? *Environ. Pollut.* 249, 610–619.
- Sendra, M., Saco, A., Yeste, M.P., Romero, A., Novoa, B., Figueras, A., 2020a. Nanoplastics: From tissue accumulation to cell translocation into *Mytilus galloprovincialis* hemocytes. resilience of immune cells exposed to nanoplastics and nanoplastics plus *Vibrio splendidus* combination. *J. Hazard. Mater.* 388.
- Sendra, M., Sparaventi, E., Blasco, J., Moreno-Garrido, I., Araujo, C.V.M., 2020b. Ingestion and bioaccumulation of polystyrene nanoplastics and their effects on the microalgal feeding of *Anemia franciscana* Ecotoc. *Environ. Saf.* 188.
- Sendra, M., Pereira, P., Yeste, M.P., Mercado, L., Figueras, A., Novoa, B., 2021. Size matters: Zebrafish (*Danio rerio*) as a model to study toxicity of nanoplastics from cells to the whole organism. *Environ. Pollut.* 268, 115769.
- Shi, Q., Fang, C., Zhang, Z., Yan, C., Zhang, X., 2020a. Visualization of the tissue distribution of fullerenols in zebrafish (*Danio rerio*) using imaging mass spectrometry. *Anal. Bioanal. Chem.* 412, 7649–7658.
- Shi, Q., Wang, C.L., Zhang, H., Chen, C., Zhang, X., Chang, X.-L., 2020b. Trophic transfer and biomagnification of fullerene nanoparticles in an aquatic food chain. *Environ. Sci. Nano* 7, 1240–1251.
- Shi, Q., Zhang, H., Wang, C., Ren, H., Yan, C., Zhang, X., Chang, X.-L., 2020c. Bioaccumulation, biodistribution, and depuration of <sup>13</sup>C-labelled fullerenols in zebrafish through dietary exposure. *Ecotoxicol Environ Saf* 191, 110173.
- Smirnova, E., Gusev, A., Zaytseva, O., Sheina, O., Tkachev, A., Kuznetsova, E., Lazareva, E., Onishchenko, G., Feofanov, A., Kirpichnikov, M., 2012. Uptake and accumulation of multiwalled carbon nanotubes change the morphometric and biochemical characteristics of *Onobrychis arenaria* seedlings. *Front. Chem. Sci. Eng.* 6, 132–138.
- Smith, C.J., Shaw, B.J., Handy, R.D., 2007. Toxicity of single walled carbon nanotubes to rainbow trout, (*Oncorhynchus mykiss*): respiratory toxicity, organ pathologies, and other physiological effects. *Aquat. Toxicol.* 82, 94–109.
- Sökmen, T.O., Sulukan, E., Türkoğlu, M., Baran, A., Özkaraca, M., Ceyhan, S.B., 2020. Polystyrene nanoplastics (20 nm) are able to bioaccumulate and cause oxidative DNA damages in the brain tissue of zebrafish embryo (*Danio rerio*). *Neurotoxicology* 77, 51–59.
- Soubaneh, Y.D., Pelletier, E., Desbiens, I., Rouleau, C., 2020. Radiolabeling of amide functionalized multi-walled carbon nanotubes for bioaccumulation study in fish bone using whole-body autoradiography. *Environ. Sci. Pollut. Res.* 27, 3756–3767.
- ASTM (American Society for Testing Materials) International, D6281-15, Standard Test Method for Airborne Asbestos Concentration in Ambient and Indoor Atmospheres as Determined by Transmission Electron Microscopy Direct Transfer (TEM), 2015.
- Stetefeld, J., McKenna, S.A., Patel, T.R., 2016. Dynamic light scattering: a practical guide and applications in biomedical sciences. *Biophys. Rev.* 8, 409–427.
- Su, Y., Yang, G., Lu, K., Petersen, E.J., Mao, L., 2017. Colloidal properties and stability of aqueous suspensions of few-layer graphene: Importance of graphene concentration. *Environ. Pollut.* 220 (Part A), 469–477.
- Su, Y., Huang, C., Lu, F., Tong, X., Niu, J., Mao, L., 2018a. Alginate affects agglomeration state and uptake of C-14-labeled few-layer graphene by freshwater snails: Implications for the environmental fate of graphene in aquatic systems. *Environ. Pollut.* 234, 513–522.
- Su, Y., Tong, X., Huang, C., Chen, J., Liu, S., Gao, S., Mao, L., Xing, B., 2018b. Green algae as carriers enhance the bioavailability of C-14-labeled few-layer graphene to freshwater snails. *Environ. Sci. Tech.* 52, 1591–1601.
- Sun, J., Petersen, E.J., Watson, S.S., Sims, C.M., Kassman, A., Frukhtbeyn, S., Skrtic, D., Ok, M.T., Jacobs, D.S., Reipa, V., Ye, Q., Nelson, B.C., 2017. Biophysical characterization of functionalized titania nanoparticles and their application in dental adhesives. *Acta Biomater.* 53, 585–597.
- Sun, X.D., Yuan, X.Z., Jia, Y.B., Feng, L.J., Zhu, F.P., Dong, S.S., Liu, J.J., Kong, X.P., Tian, H.Y., Duan, J.L., Ding, Z.J., Wang, S.G., Xing, B.S., 2020. Differentially charged nanoplastics demonstrate distinct accumulation in *Arabidopsis thaliana*. *Nat. Nanotech.* 15, 755.

- Tao, X.J., Fortner, J.D., Zhang, B., He, Y.H., Chen, Y.S., Hughes, J.B., 2009. Effects of aqueous stable fullerene nanocrystals (nC<sub>60</sub>) on *Daphnia magna*: evaluation of sub-lethal reproductive responses and accumulation. *Chemosphere* 77, 1482–1487.
- NIST, 2019. Certificate of analysis. Standard Reference Material 1566b: Oyster Tissue. <<https://www-s.nist.gov/srmors/certificates/1566B.pdf>>.
- Tervonen, K., Waissi, G., Petersen, E.J., Akkanen, J., Kukkonen, J.V.K., 2010. Analysis of fullerene-C<sub>60</sub> and kinetic measurements for its accumulation and depuration in *Daphnia magna*. *Environ. Toxicol. Chem.* 29, 1072–1078.
- Valesia, A., Parot, J., Ponti, J., Mehn, D., Marino, R., Melillo, D., Muramoto, S., Verkouteren, M., Hackley, V.A., Colpo, P., 2021. Detection, counting and characterization of nanoplastics in marine bioindicators: a proof of principle study. *Microplast. Nanoplast.* 1, 5.
- van Pomeroy, M., Brun, N.R., Peijnenburg, W.J.G.M., Vijver, M.G., 2017. Exploring uptake and biodistribution of polystyrene (nano)particles in zebrafish embryos at different developmental stages. *Aquat. Toxicol.* 190, 40–45.
- Veneman, W.J., Spink, H.P., Brun, N.R., Bosker, T., Vijver, M.G., 2017. Pathway analysis of systemic transcriptome responses to injected polystyrene particles in zebrafish larvae. *Aquat. Toxicol.* 190, 112–120.
- Waissi, G.C., Bold, S., Pakarinen, K., Akkanen, J., Leppanen, M.T., Petersen, E.J., Kukkonen, J.V.K., 2017a. Chironomus riparius exposure to fullerene-contaminated sediment results in oxidative stress and may impact life cycle parameters. *J. Hazard. Mater.* 322, 301–309.
- Waissi, G.C., Vaananen, K., Nybom, I., Pakarinen, K., Akkanen, J., Leppanen, M.T., Kukkonen, J.V.K., 2017b. The chronic effects of fullereneC(60)-associated sediments in the midge Chironomus riparius - Responses in the first and the second generation. *Environ. Pollut.* 229, 423–430.
- Waissi-Leinonen, G.C., Petersen, E.J., Pakarinen, K., Akkanen, J., Leppanen, M.T., Kukkonen, J.V.K., 2012. Toxicity of fullerene (C60) to sediment-dwelling invertebrate Chironomus riparius larvae. *Environ. Toxicol. Chem.* 31, 2108–2116.
- Waissi-Leinonen, G.C., Nybom, I., Pakarinen, K., Akkanen, J., Leppänen, M.T., Kukkonen, J.V.K., 2015. Fullerenes(nC60) affect the growth and development of the sediment-dwelling invertebrate Chironomus riparius larvae. *Environ. Pollut.* 206, 17–23.
- Wang, J., Cai, Q., Fang, Y., Anderson, T.A., Cobb, G.P., 2011. Determination of fullerenes (C60) in artificial sediments by liquid chromatography. *Talanta* 87, 35–39.
- Wang, C., Shang, C., Westerhoff, P., 2010. Quantification of fullerene aggregate nC60 in wastewater by high-performance liquid chromatography with UV-vis spectroscopic and mass spectrometric detection. *Chemosphere* 80, 334–339.
- Wang, C., Zhang, H., Ruan, L., Chen, L., Li, H., Chang, X.-L., Zhang, X., Yang, S.-T., 2016a. Bioaccumulation of C-13-fullerenol nanomaterials in wheat. *Environ. Sci. Nano* 3, 799–805.
- Wang, C., Chang, X.-L., Shi, Q., Zhang, X., 2018. Uptake and transfer of 13C-fullerenols from scenedesmus obliquus to daphnia magna in an aquatic environment. *Environ. Sci. Tech.* 52, 12133–12141.
- Wang, P., Huang, B., Chen, Z., Lv, X., Qian, W., Zhu, X., Li, B., Wang, Z., Cai, Z., 2019. Behavioural and chronic toxicity of fullerene to *Daphnia magna*: Mechanisms revealed by transcriptomic analysis. *Environ. Pollut.* 255, 113181.
- Wang, X., Liu, L., Zheng, H., Wang, M., Fu, Y., Luo, X., Li, F., Wang, Z., 2020. Polystyrene microplastics impaired the feeding and swimming behavior of mysid shrimp *Neomysis japonica*. *Mar. Pollut. Bull.* 150, 110660.
- Wang, R., Meredith, A.N., Lee Jr., M., Deutsch, D., Miadzedskaya, L., Braun, E., Pantano, P., Harper, S., Draper, R., 2016b. Toxicity assessment and bioaccumulation in zebrafish embryos exposed to carbon nanotubes suspended in Pluronic (R) F-108. *Nanotoxicology* 10, 689–698.
- Yang, M.H., Kwon, S., Kostov, Y., Rasooly, A., Rao, G., Ghosh, U., 2011. Study of the biouptake of labeled single-walled carbon nanotubes using fluorescence-based method. *Environ. Chem. Lett.* 9, 235–241.
- Zhai, G.S., Gutowski, S.M., Walters, K.S., Yan, B., Schnoor, J.L., 2015. Charge, size, and cellular selectivity for multiwall carbon nanotubes by maize and soybean. *Environ. Sci. Tech.* 49, 7380–7390.
- Zhang, L., Petersen, E.J., Huang, Q.G., 2011. Phase distribution of <sup>14</sup>C-labeled multiwalled carbon nanotubes in aqueous systems containing model solids: peat. *Environ. Sci. Tech.* 45, 1356–1362.
- Zhang, L.W., Petersen, E.J., Zhang, W., Chen, Y.S., Cabrera, M., Huang, Q.G., 2012a. Interactions of C-14-labeled multi-walled carbon nanotubes with soil minerals in water. *Environ. Pollut.* 166, 75–81.
- Zhang, W., Wang, C., Li, Z., Lu, Z., Li, Y., Yin, J.-J., Zhou, Y.-T., Gao, X., Fang, Y., Nie, G., Zhao, Y., 2012b. Unraveling stress-induced toxicity properties of graphene oxide and the underlying mechanism. *Adv. Mat.* 24, 5391–5397.
- Zhao, Q., Ma, C., White, J.C., Dhankher, O.P., Zhang, X., Zhang, S., Xing, B., 2017b. Quantitative evaluation of multi-wall carbon nanotube uptake by terrestrial plants. *Carbon* 114, 661–670.
- Zhao, L., Qu, M., Wong, G., Wang, D.Y., 2017a. Transgenerational toxicity of nanopolystyrene particles in the range of  $\mu\text{g L}^{-1}$  in the nematode *Caenorhabditis elegans*. *Environ. Sci. Nano* 4, 2356–2366.
- Zhou, R.R., Lu, G.H., Yan, Z.H., Jiang, R.R., Sun, Y., Zhang, P., 2021. Interactive transgenerational effects of polystyrene nanoplastics and ethylhexyl salicylate on zebrafish. *Environ. Sci. Nano* 8, 146–159.
- Zhu, S., Luo, F., Tu, X., Chen, W.-C., Zhu, B., Wang, G.-X., 2017. Developmental toxicity of oxidized multi-walled carbon nanotubes on *Artemia salina* cysts and larvae: uptake, accumulation, excretion and toxic responses. *Environ. Pollut.* 229, 679–687.
- Zhu, Y., Zhao, Q.F., Li, Y.G., Cai, X.Q., Li, W., 2006. The interaction and toxicity of multi-walled carbon nanotubes with *Stylonichia mytilus*. *J. Nanosci. Nanotechnol.* 6, 1357–1364.
- Zhu, B., Zhu, S., Li, J., Hui, X., Wang, G.-X., 2018. The developmental toxicity, bioaccumulation and distribution of oxidized single walled carbon nanotubes in *Artemia salina*. *Toxicol. Res.* 7, 897–906.